Monitoring and assessment of a cross-passage twin tunnel long-term performance using Wireless Sensor Network

Chao Wang[1], Miles Friedman[2] and Zili Li[3*]

[1] Civil, Structural and Environmental Engineering, University College Cork, Ireland. Email: chao.wang@ucc.ie

[2] Transport Infrastructure Ireland, Dublin, Ireland. Email: miles.friedman@tii.ie

[3] Civil, Structural and Environmental Engineering, University College Cork, Ireland. Email: zili.li@ucc.ie

***** Corresponding author

ABSTRACT: The monitoring and assessment of ageing underground tunnels is critical to ensure their serviceability, stability, and safety as arteries for a transport network in the long term. This paper first comprehensively reviewed the long-term tunnel performance monitoring case studies, aimed at highlighting the limited field monitoring data and identifying research gaps. It was found that previous studies largely focused on the performance of single tunnel sections subject to short-term disturbances (e.g., adjacent excavation), whereas limited efforts concentrated on the long-term performance of twin tunnels, let alone those with cross passages, under the influence of deteriorations. To this end, a Wireless Sensor Network (WSN) was deployed at a critical vehicle cross passage (VCP) twin tunnel section of Dublin Port Tunnel to monitor its long-term ageing performance with time, in addition to the existing long-term water leakage and lining crack monitoring. The evolvement of lining crack and water leakage since 2010 indicated the progressive deteriorations of the monitoring section, and the deployed WSN monitoring of lining inclination demonstrated a robust sensor deployment layout and monitoring plan for (quasi) real-time monitoring for a confined underground cross passage twin tunnel network. An analytical solution was proposed to convert tunnel inclination to horizontal deformation, with the converted measurements suggesting that even more than one decade after construction, both twin tunnels are still moving horizontally towards the VCP centreline in the long term, primarily due to twin tunnel interaction. Along tunnel longitudinal direction, the closer to the VCP, the greater tunnel deformation rate is, revealing the effect of cross passage on tunnel differential longitudinal behaviour, in agreement with hypotheses and numerical results in previous studies. The field observations were believed to be attributed to the two mechanisms which are hydro-geological degradation of the surrounding ground and hydro-mechanical deterioration of the tunnel, where the correlation between tunnel deformation and deteriorations was detailed.

KEYWORDS: wireless sensor network; tunnel deterioration; cross passage; twin-tunnel interaction; long-term ageing performance

INTRODUCTION

The monitoring and assessment of ageing underground tunnels is crucial to ensure their serviceability, stability, and safety status as arteries for a transport network during both construction and operation phases. In the short term, underground tunnelling process usually generates a series of loads onto a tunnel structure including earth pressure, grouting pressure, hydraulic jack thrust, thermal expansion and so on, depending on different ground conditions, construction methods, etc., which may lead to excessive tunnel deformation and structural damage. In the long term, a tunnel structure embedded in surrounding ground usually continues to deform and inevitably degrade with time during their lifespan at the risk of normal tunnel operation and serviceability (Afshani et al., 2022; Li et al., 2020; Wang et al., 2020a; Wang et al., 2022a).

Previous investigations have widely concluded that short-term tunnelling leads to ground relaxation, surface settlement, tunnel deformation, structural damage, etc., based on results from various methods such as numerical modelling and field monitoring (Afshani et al., 2020; Mair, 2008; Marshall et al., 2012; Mu et al., 2021; WONGSAROJ et al., 2013; Zhang et al., 2019; Zheng et al., 2020). On the contrary, there are limited investigations on the long-term tunnel performance, among which most studies focused on the long-term ground settlement or the long-term tunnel performance induced by external activities such as adjacent excavation (Jallow et al., 2019; Liu et al., 2020; Ng et al., 2013; Ng et al., 2022), let alone efforts on the long-term tunnel ageing/deteriorating performance (Afshani et al., 2022; Laver et al., 2017b; Li et al., 2015; Showkati et al., 2021; Soga et al., 2017b); the majority of relevant studies only focused on numerical modelling and analysis, but with scarce field data-based evidence for model or hypothesis validation.

In this study, a (quasi) real-time Wireless Sensor Network (WSN) system is deployed to a critical cross passage twin tunnel section of Dublin Port Tunnel (DPT) to monitor its long-term performance over one year and beyond. The rest of the paper is organised as follows: (1) section 2 reviews representative tunnel field monitoring cases to identify the current research gaps and validate the reliability/robustness of WSN system; (2) section 3 presents the case study of Dublin Port Tunnel WSN monitoring including an introduction of its hydrogeological and structural profile, followed by detailed WSN instrumentation; (3) section 4 gives monitoring results and an in-depth analysis of the tunnel's long-term performance and the mechanism behind the observations; (4) section 5 concludes the paper.

MONITORING OF TUNNEL LONG-TERM PERFORMANCE

Tunnel long-term deformation and/or deterioration, such as lining cracks and water leakage, has been a major engineering concern for asset owners and stakeholders owing to their potential hazards at the risk of tunnel serviceability and safety. To ensure the safe operation of ageing tunnels, field monitoring has been widely adopted as an effective approach to investigate their time-dependent deteriorating performance. Traditionally, methods like precise levelling (Ng et al., 2013), total station (Kavvadas, 2003) and wired system (e.g., vibrating wire strain gauge) (Bennett et al., 2010a) were commonly used. With technological advancement, emerging monitoring systems such as robotic total station (Zhou et al., 2020), wireless sensor network (Bennett et al., 2010b; Vanícek et al., 2009), distributed fibre optic sensing (DFOS) (Di Murro et al., 2019; Sui et al., 2021), terrestrial laser scanning (Xie and Lu, 2017; Yang and Xu, 2021), ground penetrating radar (Wang et al., 2022b), computer vision-based monitoring (Attard et al., 2021), etc., have been gradually applied to monitor the long-term behaviour of tunnels. Such advanced approaches feature automated, (quasi) real-time, temporally and/or spatially continuous sensing capability with less labour involvement in the long run. Conventional methods still remain an important option in tunnel monitoring but have been gradually complemented by these advanced innovative monitoring systems that offer higher precision and larger amounts of measurements, and simultaneously save time, labour, and cost. The following subsection reviews some representative case studies of tunnel long-term performance monitoring.

Tunnel long-term performance monitoring

Before the emergence of advanced monitoring techniques, conventional methods such as wired system and geodetic surveying played an important role in monitoring tunnel performance (Ghorbani et al., 2012). Dalgıç (2002) reported a field monitoring of the Bolu tunnel in Turkey for nearly a year using convergence and extensometers, and measurements showed an increasing deformation of the tunnel. Geodetic data on the convergence development of Ureshino tunnel line 1 in Japan also showed a continuous development of tunnel convergence during its first 5 years of service life (Guan et al., 2009). Another geodetic surveying of the convergence of a CERN tunnel since 2013 demonstrated a progressive and growing convergence with time for all six monitored cross sections (Di Murro, 2019). Ng. et al. (2013) monitored a maximum ground surface settlement of 288mm through precise levelling in Shanghai metro line 1 over a 12.5-year monitoring period and identified the main cause for the observed large tunnel settlement as the compression of the sandy aquifer due to groundwater pumping. Monsberger and Lienhart (2021) observed tunnel compression based on geodetic data of the cross-sectional deformation of the Semmering Base

Tunnel in Austria. Similarly, vibrating wire strain gauge measurements of Jubilee Line's segmental joints showed a continuously increasing tendency of joint propagation during a six-month monitoring (Bennett et al., 2010a). Kovačević et al. (2021) reported an increasing development of tunnel crown deformation during a 15-year micrometre monitoring of tunnel Pećine in Croatia. Having been successfully utilised and applied for decades, these conventional tunnel performance monitoring techniques are becoming increasingly unsuitable as they fail to satisfy the ever increasingly stringent and rigorous tunnelling project requirements, for example, less labour and cablings, real-time and continuous monitoring. Additionally, their point-based nature and heavy reliance on human operators fail to produce higher levels of data quality and accuracy, and bigger amounts of data for more objective, accurate and reliable assessment of tunnel long-term performance.

In light of this, recent decades have witnessed the growing utilisation and application of the emerging advanced systems as mentioned earlier in monitoring the long-term performance of tunnels in order to facilitate the in-depth analyses and assessment of them. However, considering the ease/convenience of field data collection, processing, interpretation in such advanced systems, and the universality and extensivity of their applications, here the following part reviews previous case studies utilising only WSN and DFOS techniques in the long-term monitoring of tunnels.

DFOS monitoring tunnel long-term performance

To understand the performance of an old brick-lined Thameslink Tunnel caused by the angled excavation of new Thameslink 2000 Tunnel underneath, Soga (2008) measured its distributed strains of a 100m section using DFOS and measurements along the tunnel circumference indicated a structural elongation towards the lower new tunnel. Similarly, Gue et al. (2015) monitored the cross-sectional and longitudinal behaviour of a 50m section of an existing London Royal Mail tunnel during the construction of a new tunnel underneath and DFOS strain data revealed a vertical ovalisation cross-sectionally and an initial-hogging-but-later-sagging mode longitudinally of the monitored section. In comparison, the following studies investigated the tunnel performance in response to nearby excavations. Mohamad et al. (2012) analysed the behaviour of 12 bolted-concrete lining rings of an existing tunnel impacted by the construction of a side-by-side tunnel and DFOS strain measurements showed the distortion of the circular tunnel into an oval/ellipsoid. Later, Soga et al. (2017a) reported another case study of DFOS monitoring of the long-term performance of a Crossrail sprayed-concrete tunnel at Liverpool Street Station induced by two cross passage excavations and concluded that the impact of cross passage excavation on parent tunnel is localised around the junction perimeter. Additionally, Li et al. (2018) evaluated the DFOS data-based performance of a diaphragm wall

(D-wall) adjacent to a deep excavation at Paddington tunnel station and found that D-wall deflection increases along its depth until the pre-existing tunnel level before reversing back. Di Murro et al. (2019) assessed the ageing performance (i.e., stress conditions) of a 100m-long inclined CERN concrete-lined tunnel using DFOS strains along 8 deteriorated sections and reported a vertical tunnel ovalisation.

WSN monitoring tunnel long-term performance

In addition to DFOS, researchers have also adopted WSN over the recent decades to monitor the development of tunnel behaviour in the long term, offering (quasi) real-time condition assessment of ageing tunnels. To understand the long-term performance of an existing cast-iron tunnel in London influenced by an underneath new tunnel excavation, Alhaddad et al. (2014) introduced a multi-suit monitoring scheme, of which WSN system was adopted to investigate the differential shear and bending displacements of a 40m-long section. Likewise, Wang et al. (2021b) evaluated the long-term structural health condition of an existing tunnel during an adjacent excavation and grouting reinforcement through WSN monitoring and results showed that tunnel convergence increased during excavation but reverted back after grouting. Another similar study by Xie et al. (2018) also noted a short-term reverse in the convergence of tunnel lining rings adjacent to soil unloading area in Shanghai metro through analysing WSN measurements. To address tunnel safety concerns arising from excessive convergence induced by extreme surcharge above a Shanghai metro tunnel section, Wang et al. (2017) monitored the deformation evolvement of two segmental tunnel rings during soil grouting and WSN measurements indicated a reduction in convergence. Similarly, another WSN monitoring in a Shanghai utility tunnel by Xie and Feng (2012) noted continuous development of lining cracks/joints and tunnel differential settlements and their fluctuations were attributed to the frequently travelling of overloaded trucks along the tunnel. Unlike the aforementioned studies, the following mainly focuses on the long-term performance of tunnels primarily caused by deteriorations in the absence of adjacent construction or other relevant ground disturbances. To determine the level of deterioration of Prague metro, Vanícek et al. (2009) adopted various methods including WSN to monitor the convergence and crack development of selected deteriorated tunnel lining sections and concluded that the selected sections generally remained stable. Yin and Huang (2015) studied the effect of longitudinal settlement on the long-term performance of a shield tunnel in Shanghai metro line 1 on the basis of WSN inclination data but focused on method feasibility to assess tunnel performance along the traffic direction. To assess the structural health condition of old London tunnels, Bennett et al. (2010a) deployed a hybrid WSN system to investigate the long-term ageing behaviour of a deteriorated tunnel section of Jubilee Line and found a trend of linear inclination development within the six-month monitoring period. Similarly, another WSN monitoring of the long-term ageing behaviour of a concrete-lined transport tunnel in seasonally cold Jilin province, China by Du et al. (2017) also showed a continuous evolvement of lining deformation. Additionally, Wang et al. (2017) reported an increase in tunnel convergence in summer but a reverse-back in winter through WSN monitoring data in a section of Shanghai Dalian road shield tunnel.

To generalise the characteristics of tunnel long-term performance monitoring, Table 1 summarises some of the representative applications of adopting both traditional and the two methods (DFOS and WSN) to monitor the structural health condition of operational tunnels, with an intention to identify the research gaps in and highlight the significance of the long-term performance monitoring and assessment of ageing tunnels. It can be concluded from Table 1 that (1) most of the previous studies focused on the performance of an existing tunnel subject to adjacent disturbances, with only a few efforts concentrating on deterioration-caused tunnel behaviour; (2) the duration of the monitoring cases by advanced methods remained relatively short, compared to monitoring by traditional approaches, failing to reflect the time-dependent long-term tunnel response; (3) all monitoring cases only applied the adopted monitoring system in a single tunnel section, with no field data on the post-construction twin tunnel interaction-caused tunnel performance, let alone the behaviour of twin tunnel section with cross passages; (4) the deterioration-motivated monitoring cases listed in Table 1 provided insights into long-term tunnel ageing behaviour but failed to address the mechanisms behind the obtained observations. Therefore, it is necessary and imperative to investigate the long-term performance of ageing tunnels under the influence of deteriorations on the basis of field monitoring measurements, assess their structural health conditions and reveal the underlying mechanisms.

Table 1. Representative cases of tunnel long-term performance monitoring

Comparison of previous monitoring data

Before commencing the long term WSN monitoring in DPT, validating the reliability/robustness of the monitoring system is essential to ensure an effective and successful endeavour in the tunnel. One easy, clear, and straightforward way is to compare previous monitoring results. Figure 1 presents the range of inclination/deformation development rate recorded in previous studies (e.g., Table 1).

Figure 1. Rate of recorded inclination/convergence development

Figure 1 shows the relatively greater variation in inclination and convergence during short term (Wang et al., 2017; Wang et al., 2021b; Xie et al., 2018) than that recorded in a comparatively longer monitoring duration (Bennett et al., 2010a; Du et al., 2017; Wang et al., 2017; Xie et al., 2018; Xie and Feng, 2012). For monitoring lasting longer than four months, results showed their inclination changes were comparable as they fell within a range of [0.000, 0.100] °/month. A similar conclusion can be drawn for convergence results that they fell within a range of [0.000, 1.303] mm/month for relatively longer monitoring. However, according to Figure 1, even though many studies highlighted the importance of long-term tunnel ageing behaviour, few of the cases adopting advanced WSN and DFOS monitoring techniques provided sufficient field monitoring data over a year, except for those cases with traditional monitoring approaches (indicated by hollow red symbols in Figure 1). For example, the WSN monitoring conducted by Bennett et al. (2010a), Du et al. (2017) and Wang et al. (2021b) only lasted between 4 to 6 months, which failed to reveal the consistent long-term tunnel deterioration performance on a yearly basis to minimise the seasonal influence. In addition, nearly none of the previous investigations discussed the mechanism behind their field observations and seldom assessed tunnel structural health conditions. Therefore, it is imperative to carry out long-term performance monitoring of ageing tunnels using the advanced methods so as to gain more accurate and in-depth assessment of tunnel performance and most importantly reveal the mechanisms.

DUBLIN PORT TUNNEL MONITORING

Considering the research gap in previous investigations, this paper conducts a dedicated case study of long-term cross passage twin tunnel performance monitoring at Dublin Port Tunnel over one year. In this tunnel, deteriorations, mainly lining cracks, water leakage and concrete spalling, have been observed to develop with time since operation (see detailed tunnel profile in the following subsections), especially around one vehicle cross passage section (i.e., VCP 16) located at the lowest elevation along the whole tunnel alignment (Wang et al., 2020b, 2021a), as shown in Figure 3(*a*). These deteriorations have caused concerns over their influence on tunnel serviceability and safety to engineers and asset owners. In the light of asset owner's requirements (e.g., no frequent visits to the tunnel) and the onsite tunnel configurations (e.g., tunnel clearance, engineering hours, tunnel maintenance activities, etc.), Wireless Sensor Network is chosen as the technology to deliver DPT monitoring objectives, which will be detailed later.

Dublin Port Tunnel profile

Dublin Port Tunnel was constructed firstly to alleviate air pollution, traffic congestion and road safety concerns caused by Heavy Goods Vehicles frequently travelling within the city and secondly to provide better connectivity between Dublin Port and the rest of the city (see Figure 2(*a*) for DPT location). The 5.6km-long two-direction dual-carriageway twin tunnel is comprised of four distinctive sections which are northern and southern cut-and-cover sections (C&C), middle bored section and one specialised pipe-jacked section under the Dublin-Belfast railway line, as illustrated in Figure 2(*b*). The tunnel alignment has the deepest stretch of up to 34m below the surface ground at the mid-section and a gradual rise out to the ground level at both the north and south ends (Skipper et al., 2005). To better accommodate emergency requirements, tunnel cross passages were constructed along the alignment to aid the evacuation of tunnel users and the movement of vehicles, with fifteen pedestrian cross passages situating about 250m apart and four vehicle cross passages at around 1,000m intervals accompanied by laybys and emergency and recovery areas. Two of the VCPs are located within the bored tunnel section while the other two in the C&C sections respectively. The VCPs and laybys were constructed from the main bored tunnel after the passage of the TBMs.

Figure 2. **Location and alignment of Dublin Port Tunnel**

DPT Geological profile

This four-section tunnel encounters different geological stratigraphy at different section depths. The geological succession pertaining to the northern and southern C&C sections showed that these two sections were predominantly excavated through the following three general ground layers: made ground, glacial sands and gravels, and glacial till (locally Dublin Boulder Clay), whilst the bored tunnel section in the middle mainly was located in argillaceous calcisiltite (limestone). The VCP 16 section, the main subject of this study, is at the lowest point along the tunnel longitudinal alignment, as shown in Figure 3(*a*). It is a section of particular interest due to observed critical tunnel deformation and deterioration such as water leakage, lining cracks and concrete spalling. With reference to the face-logs collected prior to tunnel excavation, the nearest available borehole logs, and previous studies on the geology around DPT (Kovacevic et al., 2008; Long and Menkiti, 2007; Skipper et al., 2005), a simplified vertical ground profile around VCP 16 section is given in Figure 3(*b*). The VCP 16 tunnel section is approximately 20m below ground surface in argillaceous limestone (G3), with two overlying soil layers of sandy clayey gravel (G1) and sandy gravelly clay (G2) which can be generally categorised into "Dublin Boulder Clay" based on previous investigations (Cabarkapa et al., 2003; Kovacevic et al., 2008; Lawler et al., 2010). This dense, stiff, and low-permeability soil overlies much of Dublin City, including the DPT region, as the primary superficial glacial deposit. It was previously treated as a cohesive soil. More recent studies by Trinity College Dublin and University College Dublin suggested that it was more practical to view it as a frictional material based on extensive laboratory tests (Long and Menkiti, 2007). The bedrock layer argillaceous calcisiltite is highly interbedded with thin to thick black argillaceous shale.

Figure 3. VCP 16 section geological profile

DPT Hydraulic profile

As an underground urban road tunnel, Dublin Port Tunnel is equipped with a full set of waterproofing and drainage system. The 2.63km-long bored tunnel section in this study structurally consists of annular grout, segmental lining, and cast-in-situ secondary lining, with two waterproofing membranes installed in-between the three structural layers and drains constructed to aid the discharge of groundwater, as shown in Figure 4(*a*). Groundwater drainage for the bored tunnel section flows towards the main drainage sump buried underneath the invert of each bore at VCP 16 section, as shown in Figure 3(*a*). The twin-bore tunnel was designed to be watertight throughout its service lifetime, with an initial permeability of 2.0×10^{-13}m/s for tunnel lining segments. On opening in 2006, the tunnel was found to have water ingress at several locations including VCP 16 section. Repairs comprised replacing the waterproofing membranes and lining concrete locally. Subsequent inspections and maintenance works indicated that tunnel lining deteriorations (e.g., lining cracks and water infiltration) have gradually developed with time, as noted in Figure 4(*b*). Recent years have also witnessed progressive development of the deteriorations, causing a critical engineering concern for tunnel maintenance. Therefore, a WSN monitoring system, as mentioned in Section 2.1, is adopted to monitor the long-term performance of such twin-tunnel cross passage section under the influence of deteriorations.

Figure 4. DPT hydraulic profile

WSN monitoring instrumentation

On account of Dublin Port Tunnel's ongoing progressive deteriorations observed onsite, a long-term monitoring project using WSN was launched with an aim to assess its long-term health condition and to reveal the mechanism behind its time-dependent ageing behaviour even after more than a decade's operation. An existing crack monitoring scheme is introduced before detailing the WSN instrumentation at VCP 16 section of the tunnel.

Existing crack monitoring

Concrete cracks have been identified at many locations of the secondary lining along the whole tunnel alignment a few years after opening. A manual crack monitoring system has been in place since 2010 to monitor the development of some major lining cracks. This method measured the distance change between the centre of stainless-steel crack monitoring discs attached to both sides of a crack using a calliper, as shown in Figure 5.

Figure 5. Existing crack monitoring

The measurements were taken on a monthly basis and logged to a data sheet for engineers to review. Comparisons with previous records were provided for each subsequent data reading so that engineers could know if the crack development still fell within the allowable threshold of 0.3mm set out by safety requirements. However, it should be noted that such monitoring is inevitably inaccurate, time- and labour-consuming and most importantly carries strong subjectivity in terms of manual measurement, necessitating more reliable automatic monitoring. Thus, a WSN monitoring system is adopted and introduced in the following sections.

WSN onsite deployment

Monitoring location

The existence of VCP for one thing serves emergency purposes but for another also poses a risk to the integrity of the twin tunnel section as it creates an opening along the tunnel alignment. Such opening makes VCP sections more structurally critical than typical intact bored tunnel sections (Li et al., 2015). In comparison with other VCP sections and non-VCP sections, VCP 16 section is chosen as the monitoring section of interest due to its relatively extensive deteriorations. Theoretically, the structural performance of the near-VCP 16 areas is of more significance as they connect the cross passage and twin tunnels. Besides, the section where the bored tunnel and layby tunnel connect should also be taken into account as one of the monitoring locations because of the transition of tunnel geometry from non-circular layby tunnel to circular bored tunnel (as shown in Figure 6(*a*)).

Monitoring objectives

The progressively developing tunnel deteriorations cause concern over its serviceability and safety in the long term. By conducting structural health monitoring of Dublin Port Tunnel, the project aims to (1) enhance the understanding of this tunnel's aging performance for tunnel inspection and maintenance; (2) reveal the impact of deterioration on the behaviour of the twin-tunnel cross passage section; (3) offer field data-based evidence to quantitatively validate the assumptions or hypotheses proposed by previous investigations on long-term tunnel performance; (4) reveal the mechanisms behind tunnel long-term performance based on field measurements.

Sensor onsite deployment

A package of WSN sensors and nodes sourced from Wisen Innovation UK Ltd were deployed on tunnel linings of the critical VCP 16 section. Table 2 presents the list of sensors adopted. Figure 6(*a*) gives the detailed illustration of the sensor onsite deployment. In the northbound tunnel, three tilt-meters were deployed on a ring (R1) located at a deteriorated section of bored tunnel around 3.0m from the northern end of the layby tunnel. On the "incomplete" central ring (R2) of layby tunnel, another three inclinometers were also deployed due to stability concerns caused by the existence of VCP 16 opening, with one just above the opening and the other two on the other side of lining wall. In the southbound tunnel, a similar deployment of inclinometers was carried out around the VCP 16 section. Three tilt-meters were installed on the "incomplete" central ring (R3) of layby tunnel while another four deployed on a ring (R4) located about 1.2m from the northern end of southbound layby tunnel. The reason why inclinometers were deployed on the central ring of layby tunnel is because based on theoretical and numerical analysis, the central part of the layby tunnel intersecting the VCP 16 opening is anticipated to develop the maximum deformation (Epel et al., 2021; Wu et al., 2020). The other two non-central rings of WSN inclinometers were deployed based on the deteriorations of this tunnel section where cracks, water leakage and concrete spalling were observed. Figure 6(*b*) shows the practical deployment of sensors. In addition to inclinometers, two crack-meters were installed on the two rings in the southbound tunnel and connected to the vibrating wire interface node which was mounted between these two crack-meters, see Figure 6(*a*). The sensor nodes were installed above the tunnel washing dividing line (about 4m above road surface) due to concerns over possible destabilisation to the sensors caused by regular tunnel wall maintenance wash. Sensors that were installed just a bit above the dividing line are at a height of around 4.20m (T1, T4, T9, T10 and T13) from road surface, with the nodes higher up at a height of around 6.00m (T2, T3, T5, T8, T11 and T12). For the two sensor nodes (T6 and T7) installed above the VCP 16 opening at the central layby tunnel, the height is about 5.50m from road surface.

Table 2. List of WSN sensors and nodes

Figure 6. WSN sensor deployment

WSN system performance

A sampling frequency of every 60mins is applied to all sensor nodes considering the rate of tunnel deformation, and the data transmission cycle from the gateways to the remote server is set as every six hours in order to maximise the usage of batteries and also to avoid frequent battery replacement. Data transmission for each cycle is set to complete within a 2-minute period. During monitoring, all collected data can either be communicated to sensor nodes themselves or to the remote server wirelessly for different levels of users to review, download, manage and utilise. Such wireless communication links between WSN sensors, gateways and remote server normally follow different topology configurations (e.g., star, mesh and clustered topology) in different case studies (Rodenas-Herráiz, 2016). In DPT project, the WSN sensors formed a star topology, as shown in Figure 7, due to the small scale of the network. Onsite tests showed that sensors deployed in the northbound tunnel could only communicate with gateway G1 deployed in the northbound as the steel gate located in the middle section of VCP 16 and tunnel structure block the signal transmission (disrupt the communication range) between sensors in the north-bore and the gateway in the south-bore (G2), indicating that WSN system robustness and redundancy should be taken into consideration when undertaking underground tunnel monitoring.

Figure 7. WSN star topology in Dublin Port Tunnel

WSN MONITORING RESULTS

Crack development

Results from the existing crack monitoring during the period from 2010 to 2018 were presented in Figure 8 where the development means the incremental crack width difference between the baseline reading in April 2010 and the subsequent readings. It shows that since the start of crack development monitoring, all the monitored cracks showed either propagation or shrink variations and almost all of them fell within the threshold of 0.3mm during the 8-year period, except for a few monitoring locations near the VCP 16 section (e.g., crack monitoring point 42, 44 and 46). Generally, the propagation of cracks for the rest of the tunnel during this period remained minor whilst for those concentrated around VCP 16 section their development of exceeding the allowable threshold of 0.3mm should be given prioritised attention, as such progressive lining crack development facilitates groundwater leakage through cracks in lining concrete, as evidenced in Figure 4(*b*) and Figure 5. This in turn could further deteriorate the tunnel structure through for example lining erosion, reducing the lining bearing capacity and subsequently causing more cracks and deformation. The repeated chain of deteriorating actions threatens the safety of tunnels, necessitating the long-term monitoring of the ageing performance of the selected tunnel section.

Figure 8. Crack development from existing monitoring

Lining deformation

Inclination development

Figure 9 shows lining inclination development for tunnel rings R1, R2, R3 and R4 during the first one and half years of monitoring from April 2021 to November 2022. Positive values of inclination mean anticlockwise rotation of tilt meters while negative values mean clockwise rotation. In Figure 9, it can be seen that almost all sensors at different locations of the VCP section are showing inclination development over the year. That is, the tunnel is still deforming with time even after more than a decade of operation and in the absence of ground disturbances nearby. It is worthy of noting that sensors T1 and T2 stopped transmitting data in March 2021. After remote investigation into the cause of their dysfunction by engineers from the manufacturer, battery consumption was rooted out for causing the failure and the cause is believed to be a problem of the sensor data transmission unit. For ring R1, the inclination of the sensing locations (T1, T2 and T3) experienced an increase from April 2021 to September 2021 and from April 2022 to September 2022, followed by a decrease from September 2021 to April 2022 and September 2022 onwards, and the rotation of lining ring was counterclockwise. Upon comparison, the inclination development of the four sensing locations on R4 (T10, T11, T12 and T13) generally had an opposing tendency as that of the locations on R1 and a clockwise rotation of the tunnel lining ring. For the other two central rings, sensing locations on R2 experienced a similar development of inclination and rotation (counterclockwise) as the sensing locations on R1 except for T6 where an opposing trend and rotation (clockwise) was observed. Lining ring R3 witnessed a clockwise rotation of the three sensing locations. During the monitoring period, the variation of the inclination development was believed to be caused by the seasonal effect, and the increase of inclination from the start to the end was due to the ongoing tunnel deterioration including lining cracks and water leakage. However, to gain an understanding of the full picture of this tunnel section's deformation, an even longer period of monitoring will be analysed in the future to check the seasonal fluctuations.

Figure 9. Tunnel inclination development with time (monthly increment)

For better graphical representation of tunnel lining deformation, Figure 10 summarises the rate of inclination development and rotation of monitoring locations on the four tunnel rings. It is obvious that for the two rings located in central laybys of the twin tunnels, the rotations of monitoring locations on R2 (anticlockwise) and R3 (clockwise) are generally symmetrical, except for tilt meter T6. Similarly, R1 (anticlockwise) and R4 (clockwise) also showed a symmetrical trend of lining rotation. In terms of the rate of inclination development, different locations showed different magnitudes during this period, as the values in Figure 10 suggest (blue arrow means direction of horizontal displacement). Generally, the rate for sensing locations on the two central rings R2 and R3 is comparatively greater than the rate for the similar sensing locations on the other two rings R1 and R4 during this period, except for the two sensors T6 and T7. On tunnel rings R2 and R3, the deformation rate for the sensing locations at T6 and T7 close to the VCP opening is upon comparison lower than the rate of other sensors on the same ring. However, for tunnel rings R1 and R4, the rate of inclination development for the sensing locations close to the middle ground of the twin tunnel (i.e., T3, T10 and T11) is relatively greater than the rate of other sensors on the same rings respectively. For this particular case study, some possible underlying mechanisms/explanations for these findings and the correlation between the monitored tunnel deformation and deteriorations are proposed in the following section, with an aim to gain a deeper understanding of the long-term performance of the tunnel section and to validate the previous results or hypotheses on the effect of twin tunnel interaction on tunnel long-term behaviour.

Figure 10. Rate of tunnel inclination

Horizontal deformation

The rotations shown in Figure 10 for the monitoring locations cannot directly show the deformation of the tunnel linings. Previous efforts by Shao (2019), Xie et al. (2018), Wang et al. (2021b), etc. have demonstrated the feasibility and effectiveness of converting inclination data to tunnel cross-sectional deformation (convergence) on the basis of geometrical derivation. However, they all focused on shield segmental tunnels where tunnel segments were regarded as rigid bodies and only segmental rotations of the joints were considered as the cause for horizontal convergence neglecting tunnel bending deformation. To the authors' best knowledge, no efforts have been paid to investigate the conversion from inclination to convergence for non-segmental tunnels. To this end, an attempt is made below to derive the conversion relationship between inclination and lining deformation for non-segmental tunnels.

Wood (1975) assumed that a circular tunnel ring's deformation (continuum model, as shown in Figure 11) under pure bending in elastic ground follows an "elliptical" mode and the omission of shear stresses between tunnel extrados and the surrounding ground makes tunnel deformation estimation conservative but greatly simplifies the solution. Based on the assumptions of small displacement and plain strain, the radial displacement can be estimated by the following equation:

[1] $$u = -\frac{2c(1+v)}{E_c}\left[r^{-3} - 6(1-v)r_0^{-2}r^{-1}\right]cos2\varphi$$

Hence at tunnel extrados $r = r_0$

[2] $$u_0 = -\frac{2cr_0^{-3}}{E_c}(1+v)(5-6v)cos2\varphi \text{ or } u_0 = \hat{u}_0 cos2\varphi$$

Where $\pm\hat{u}_0$=maximum radial displacement, u_0=radial displacement at tunnel extrados ($r = r_0$), u=tunnel radial movement, c= cohesion, E_c= Young's modulus, v= Poisson's ratio, φ= circumferential angle. In polar coordinate, the differentiation of radial displacement gives the incremental gradient (Li et al., 2018), which in tunnel cases is the rotation of tunnel lining. Therefore, by differentiating equation (2) by angle φ gives

[3] $$\frac{\partial u_0}{\partial\varphi} = \hat{u}_0 \times (-2sin2\varphi) = \Delta\theta$$

Where $\Delta\theta$ is the development of inclination monitored by inclinometers. Combing equations (2) and (3) obtains the analytical solution for converting lining inclination to radial deformation, as shown in equation (4).

[4] $$u_0 = -\frac{\Delta\theta}{2tan2\varphi}$$

The horizontal component of the converted radial displacement can thus be derived as:

[5] $$u_x = u_0 \times sin\varphi = -\frac{\Delta\theta}{2tan2\varphi} \times sin\varphi$$

The converted horizontal displacement of sensing locations on the tunnel rings and the direction of horizontal movement for each sensor are shown in Figure 12 and Figure 10, respectively. Results show that generally the two central tunnel rings R2 and R3 are deforming towards the VCP, so do the other two rings R1 and R4, the mechanism of which will be described in detail in the following section.

Figure 11. Plain strain continuum model

Figure 12. Converted horizontal displacement of sensing locations with time

Tunnel performance analysis

As stated earlier, many previous efforts largely focused on presenting the WSN monitoring results of a short section of a single tunnel during a short period, without considering the effect of deteriorations on the ageing performance of cross-passage twin tunnel sections in the long term, let alone the possible mechanisms behind the observations. In this section, field measurements-based evidence obtained in previous section is used to validate the hypotheses or theories by previous studies regarding twin tunnel interaction and cross passage, and the correlation between the observed deformation and tunnel deteriorations (mechanism) is analysed thereafter.

Twin tunnel effect

Twin tunnel interaction has been identified as a major factor influencing the performance of tunnels during both construction and operation phases. During tunnel construction, ground softening around twin tunnels leads to a stiffness reduction (particularly the double-softened ground in-between the two tunnels) (Zhang et al., 2019) and subjects the middle ground to stress redistribution (Laver et al., 2017a), causing the retraction of horizontal support from the middle ground to the twin tunnels (Epel et al., 2021; Li et al., 2015) and subsequent greatest bending moment at tunnel sections close to the ground under interaction and afterwards the asymmetrical tunnel deformation (Epel et al., 2021) as illustrated in Figure 13(*a*).

Similarly, in Dublin Port Tunnel, construction records showed that the construction of the northbound tunnel preceded the southbound excavation. The load transfer from the first tunnel construction to the second induces an increase in tunnel internal forces (bending moments and axial force) at tunnel sections that are close to the middle ground (Ng et al., 2004), theoretically leading to asymmetrical deformation of the twin tunnels before long-term operation. In the long term, soil column I consolidates more rapidly between the twin tunnels than soil columns II/III as column I has a shorter drainage path towards the twin tunnels (underground water in column I flows towards both tunnels while water in column II/III flows towards the right/left tunnel only) (Li et al., 2015; Soga et al., 2017b), as shown in Figure 13(*b*). This causes further retracting of the horizontal support for the tunnel sections close to column I and thus leading to an increasing horizontal movement of tunnel linings towards column I, as demonstrated and validated by field monitoring results in Figure 10 and Figure 12.

Figure 13. Twin tunnel effect

Vehicle cross passage effect

Vehicle cross passages are normally constructed after completing the twin tunnels (Epel et al., 2021; Li et al., 2015). Many researchers have concluded the significance of VCP on twin tunnel performance. Before VCP construction, the interaction of the northbound and southbound arches causes a vertical stress concentration in column I, leading to asymmetrical squatting of the twin tunnels, with greater horizontal deformation at tunnel spring-line towards the VCP for the sides of the tunnels that are close to column I (see Figure 13). During VCP construction, its advance breaks the balance of the twin ground arches around the VCP area (Figure 14(*a*)), forcing a third load redistribution in the surrounding ground. Soil column I's share of overburden increases as the advance of VCP, and the forming of the VCP arch transfers part of the overburden to the area in the two sides of the VCP cross section. The excavation of VCP instigates further asymmetrical squatting of the twin tunnel sections that are close to the opening as the lateral ground support in the interaction zone is gradually removed.

After VCP construction, the existence of its structure changes the share of the overburden on the twin tunnels. To illustrate the ground arching mechanism above the cross-passage twin tunnel, Li et al. (2015) proposed a "table" load column analogy, as shown in Figure 14(*b*). As mentioned, the short-term VCP excavation activity breaks the balance of twin tunnel arching, together with the forming of new VCP arch, enabling the transfer of overburden to the areas in the two sides of VCP cross section and twin tunnels, which are column II and IV as in Figure 14(*b*) due to symmetry, with the generation of large excess pore water pressure. In the long term, as pore water pressure dissipates, ground columns II and IV also retract support (faster retraction from column IV as it supplies groundwater to twin tunnels), leading to an increasing share of overburden on twin tunnel linings, especially on the sides closest to the ground in between. Such stress redistribution and load transfer in the long term leads to faster deformation of tunnel cross passage sections than that of normal non-VCP twin tunnel sections, which can be validated by the rate of horizontal displacement of sensing locations converted from inclination data in Figure 10 and Figure 12. In general, the deformation rate at R2 and R3 (VCP twin tunnel) is larger than the rate at R1 and R4 (non-VCP twin tunnel), except for the deformation rate at sensing locations T6 and T7 whose rate is lower than other sensing locations on the same ring (T4 and T5 on ring R2, T8 and T9 on ring R3). This field observation shows a good agreement with the load column analogy in Figure 14. Compared to non-VCP twin tunnel sections, the sensing locations close to the VCP opening, horizontally pushed by soil loading, is prone to deforming back due to the reduction in its horizontal stiffness (Li et al., 2015), leading to a lower deformation rate for sensing locations at T6 and T7 as evidenced in Figure 10.

Figure.14. Illustration of VCP effect

Correlation between tunnel deformation and deteriorations

The monitored observations reveal the effect of twin tunnel interaction and the effect of cross passage on the long-term performance of the deteriorated tunnel section, which were in line with previous theoretical and numerical analyses. However, the correlation between the ongoing progressive long-term tunnel deformation even a decade after construction and the observed deteriorations is yet to be investigated. This subsection specifically analyses the correlation from both qualitative and quantitative perspectives.

Water leakage and deformation

Routine onsite observations and inspections have found that some intruding dark ground particles were transported into VCP 16 section tunnel lining with groundwater ingress through cracks and drains, as evidenced in Figure 4(*b*), indicating ground erosion and/or weathering behind tunnel linings (Meguid and Dang, 2009; Sandrone and Labiouse, 2010; Showkati et al., 2021). In the long run, theoretically, such water ingress and ground degradation, as concluded by many previous studies (Sandrone and Labiouse, 2010; Showkati et al., 2021; Wang et al., 2021c), leads to a decrease in the strength and mechanical properties of rock masses, and an increase in ground pressure acting on tunnel lining. Consequently, a resultant increase in tunnel axial thrust, bending moment and subsequent deformation is imminent. A prior study by the authors Wang et al. (2022a) concluded that the current hydraulic status of the tunnel was found to be partially permeable after more than a decade's operation compared to the initial watertight status of DPT, as indicated in Figure.15(*a*). The qualitative evidence shown in Figure 4 and Figure 5 and the quantitative analyses in Wang et al. (2022a) have also shown the development and propagation of hydraulic deterioration in DPT, which could (1) expedites the twin tunnel effect: increasing horizontal deformation towards the VCP centreline due to an increasing share of load acting on twin tunnel linings close to ground column I in Figure 13(*b*); (2) and also expedites the VCP effect: increasing deformation occurs at VCP twin tunnel sections than non-VCP ones through an increasing share of overburden bored by columns II and IV in Figure 14(*b*). However, the monitored water flow of DPT also showed that hydraulic deterioration appeared to have slightly slowed done since 2016, indicating that it may not be the exclusively dominant factor for the ongoing tunnel deformation captured by WSN measurements.

Crack and deformation

Many previous studies have summarised that both hydraulic and structural deteriorations reduce the capability of tunnel lining to resist external loads, consequently jeopardizing tunnels' mechanical (e.g., axial thrust and bending moment) and deformational performance in the long term (e.g., convergence and deformation) (An and Song, 2019; Usman and Galler, 2013; Závacký et al., 2018).

For VCP 16 section of DPT, existing field measurements on crack development and the crack density distribution can provide some quantitative evidence to understand the ongoing tunnel deformation. By adopting the approach of deep learning, the crack distribution on tunnel side walls can be automatically detected and calculated after model training. Due to the limited space in this paper, only one sidewall of the monitored section was chosen for demonstration. Figure.15(*b*) presents the crack distribution along the layby enlargement side of the northbound of the selected section following automatic detection through deep leaning. It is apparent that most of the lining cracks can be classified as vertical cracks (circumferential cracks) while some as diagonal cracks (oblique cracks) (O'Brien et al., 2023), in line with previous findings that vertical crack is the dominant type of tunnel cracks (Wang et al., 2018; Xu et al., 2020). The cause of these vertical cracks may possibly be attributed to longitudinal bending-induced differential deformation of the tunnel section. In addition, Figure.15(*b*) clearly shows that the crack density around the central area of the layby tunnel (VCP-section) is higher than that of the two ends of the layby tunnel (non-VCP section), suggesting greater reduction of lining strength and stiffness around the central layby area, and thus greater subsequent increase in tunnel internal forces and deformation. This consolidates the aforementioned vehicle cross passage effect and verifies that the VCP-section is more structurally critical than non-VCP sections.

Therefore, it is reasonable to conclude that the combined effect of both hydraulic and mechanical deterioration of tunnel linings, based on the qualitative observation and quantitative evidence of both water leakage and concrete cracks, plays a key role in causing the progressive long-term tunnel deformation. The propagation of mechanical deterioration (i.e., concrete cracks) aggravates hydraulic deterioration (i.e., a growing amount of water leakage into the tunnels), and in turn, the development of hydraulic deterioration also exacerbates mechanical deterioration, contributing to the ongoing tunnel deformation, as recorded by WSN measurements.

Figure 15. (*a*) *RP* for DPT *vs. DS*; (*b*) Layby lining crack distribution

CONCLUSIONS

Long-term performance of ageing tunnels plays a significant role in the assessment and evaluation of their structural health conditions. This paper investigates the long-term structural performance of a cross-passage twin tunnel under the influence of deteriorations using Wireless Sensor Network field monitoring. It was found in this study that the WSN system is required to be robust in harsh underground environment, durable for long-term monitoring and intelligent to self-adapt/self-configure in unfavourable situations so as to deliver the monitoring objectives set out for such monitoring projects. The main conclusions can be drawn as follows:

(1) Previous tunnel monitoring results indicated that the long-term tunnel inclination rate generally fell within a range of [0.000, 0.100] °/month, while the long-term tunnel deformation rate was within a range of [0.000, 1.303] mm/month. Although small compared to short-term tunnel deformation due to construction, the long-term tunnel

ageing deformation may accumulate with time and even exacerbate beyond the threshold limit, posing a risk to tunnel safety/serviceability for traffic resilience.

(2) The existing crack monitoring results showed that some cracks around the tunnel section of interest have propagated over its threshold of 0.3mm, indicating the progressive deteriorations around this area instead of the whole tunnel, and the deployed WSN monitoring of lining inclination demonstrated a robust sensor deployment layout and monitoring plan for (quasi) real-time monitoring for a confined underground cross passage twin tunnel network.

(3) Field inclination measurements showed that the tunnel is still deforming with time even after more than a decade's operation. A method was proposed to convert inclination data to horizontal deformation for continuous cast-in-place concrete tunnel lining, and the converted deformation indicated that: 1) In terms of deformation mode, both the two tunnels are moving towards the twin tunnel centreline, and 2) for the magnitude of deformation, along the longitudinal direction, the two tunnel central rings R2 and R3 closer to the VCP were generally deforming at a faster rate than that for the other two R1 and R4 at a distance away from the VCP. The observed deformation is likely to further develop as the tunnel continues to deteriorate with time.

(4) The ground column I between the twin tunnels consolidates at a faster rate than that of the ground columns at the sides. It caused reduction in the horizontal support for the tunnel sections close to column I, thus leading to an increasing horizontal movement of tunnel linings towards twin tunnel centreline. In addition, the presence of VCP removes the soil column between twin tunnels and leads to new load transfer patterns onto the twin tunnel structure in the long term; an increasing share of overburden on twin tunnel linings close to the VCP contributes to a faster deformation of tunnel cross passage sections (R2 and R3) than that of normal non-VCP twin tunnel sections (R1 and R4). The field measurements in this study show that the effects of twin tunnel interaction and cross passage on tunnel behaviour in agreement with hypothesis and numerical results in previous studies.

(5) Qualitative and quantitative analyses jointly demonstrated an interconnected correlation between the field deformation measurements (e.g., WSN data) and observed tunnel deterioration like water leakage and lining cracks. The propagation of mechanical deterioration (i.e., cracks) aggravates hydraulic deterioration (i.e., a growing amount of water leakage into tunnels), and in turn, the development of hydraulic deterioration also exacerbates mechanical deterioration, contributing to the ongoing tunnel deformation, as recorded by WSN measurements.

In summary, this case study of Dublin Port Tunnel clearly demonstrated the capability of WSN for robust, durable and intelligent long-term tunnel monitoring. The WSN field measurements reveal the effect of VCP on twin tunnel behaviour in both the transverse and longitudinal directions, validating hypothesis and numerical results in previous studies. In addition, the comparison between WSN field deformation measurements and observed tunnel defects (e.g., crack, water leakage) demonstrates the interaction between hydraulic deterioration and mechanical one. The generic findings and conclusions in this study, particularly inclination-deformation conversion, the twin tunnel interaction and vehicle cross passage effect and the underlying mechanisms, can provide reference for the long-term performance assessment of other tunnels in different ground conditions.

DECLARATION OF COMPETING INTEREST

The authors declare that they have no known competing financial interests or personal relationships that could have appeared to influence the work reported in this paper.

DATA AVAILABILITY STATEMENT

Some or all data, models, or code that support the findings of this study are available from the corresponding author upon reasonable request.

ACKNOWLEDGEMENT

This work is jointly funded by Irish Centre for Research in Applied Geosciences of Science Foundation Ireland and Transport Infrastructure Ireland. The contribution of geotechnical reports and field monitoring data from Geological Survey Ireland and Egis Road and Tunnel Operation and the efforts made by Professor Mike Long from University College Dublin in facilitating the project are also greatly appreciated. This research is also partly sponsored by the National Natural Science Foundation of China (No. 51978530).

REFERENCES

Afshani, A., Akagi, H., Konishi, S., 2020. Close construction effect and lining behavior during tunnel excavation with an elliptical cross-section. Soils and Foundations 60, 28-44.

Afshani, A., Li, W., Oka, S., Itoh, Y., Akagi, H., 2022. Study of the long-term behavior of segmented tunnels in cohesive soil based on the circumferential joint opening. Tunnelling and Underground Space Technology 120, 104210.

Alhaddad, M., Wilcock, M., Gue, C.Y., Bevan, H., Stent, S., Elshafie Mohammed, Z.E.B., Soga, K., Devriendt, M., Wright, P., Waterfall, P., 2014. Multi-suite monitoring of an existing cast iron tunnel subjected to tunnelling-induced ground movements. Tunneling and Underground Construction, 293-307.

An, J.-S., Song, K.-I., 2019. Back analysis of an operating subsea tunnel considering the degradation of ground and concrete lining. Marine Georesources & Geotechnology 37, 517-523.

Attard, L., Debono, C.J., Valentino, G., Di Castro, M., 2021. Vision-Based Tunnel Lining Health Monitoring via Bi-Temporal Image Comparison and Decision-Level Fusion of Change Maps. Sensors 21.

Bennett, P.J., Kobayashi, Y., Soga, K., Wright, P., 2010a. Wireless sensor network for monitoring transport tunnels. Proceedings of the Institution of Civil Engineers - Geotechnical Engineering 163, 147-156.

Bennett, P.J., Soga, K., Wassell, I.J., Fidler, P.R.A., Abe, K., Kobayashi, Y., Vanícek, M., 2010b. Wireless sensor networks for underground railway applications: case studies in Prague and London. Smart Structures and Systems 6, 619-639.

Cabarkapa, Z., Milligan, G.W.E., Menkiti, C.O., Murphy, J., Potts, D.M., 2003. Design and performance of a large diameter shaft in Dublin Boulder Clay, BGA International Conference on Foundations: Innovations, observations, design and practice, pp. 175-185.

Dalgıç, S., 2002. Tunneling in squeezing rock, the Bolu tunnel, Anatolian Motorway, Turkey. Engineering Geology 67, 73-96.

Di Murro, V., 2019. Long-term performance of a concrete-lined tunnel at CERN, Department of Engineering. University of Cambridge, Cambridge, UK.

Di Murro, V., Pelecanos, L., Soga, K., Kechavarzi, C., Morton, R., Scibile, L., 2019. Long-term deformation monitoring of CERN concrete-lined tunnels using distributed fibre-optic sensing. Geotechnical Engineering Journal of the SEAGS & AGSSEA 50, 1-7.

Du, F., Zhang, D., Wu, Y., Huang, H., Sun, F., 2017. WSN-based health monitoring of highway tunnel lining in seasonal cold region, The 2017 World Congress on Advances in Structural Engineering and Mechanics (ASEM17), IIsan (Seoul), Korea.

Epel, T., Mooney, M.A., Gutierrez, M., 2021. The influence of face and shield annulus pressure on tunnel liner load development. Tunnelling and Underground Space Technology 117, 104096.

Ghorbani, M., Sharifzadeh, M., Yasrobi, S., Daiyan, M., 2012. Geotechnical, structural and geodetic measurements for conventional tunnelling hazards in urban areas – The case of Niayesh road tunnel project. Tunnelling and Underground Space Technology 31, 1-8.

Guan, Z., Jiang, Y., Tanabashi, Y., 2009. Rheological parameter estimation for the prediction of long-term deformations in conventional tunnelling. Tunnelling and Underground Space Technology 24, 250-259.

Gue, C.Y., Wilcock, M., Alhaddad, M.M., Elshafie, M.Z.E.B., Soga, K., Mair, R.J., 2015. The monitoring of an existing cast iron tunnel with distributed fibre optic sensing (DFOS). Journal of Civil Structural Health Monitoring 5, 573-586.

Jallow, A., Ou, C.-Y., Lim, A., 2019. Three-dimensional numerical study of long-term settlement induced in shield tunneling. Tunnelling and Underground Space Technology 88, 221-236.

Kavvadas, M., 2003. Monitoring and modelling ground deformations during tunnelling, Proceedings of the 11th FIG symposium on deformation measurements, Greece.

Kovačević, M.S., Bačić, M., Gavin, K., Stipanović, I., 2021. Assessment of long-term deformation of a tunnel in soft rock by utilizing particle swarm optimized neural network. Tunnelling and Underground Space Technology 110, 103838.

Kovacevic, N., Miligan, G.W.E., Menkiti, C.O., Long, M., Potts, D.M., 2008. Finite element analyses of steep man-made cuts in Dublin boulder clay. Canadian Geotechnical Journal 45, 549-559.

Laver, G., Li, Z., Soga, K., 2017a. Method to Evaluate the Long-Term Surface Movements by Tunneling in London Clay. Journal of Geotechnical and Geoenvironmental Engineering 143, 06016023.

Laver, R.G., Li, Z., Soga, K., 2017b. Method to Evaluate the Long-Term Surface Movements by Tunneling in London Clay. Journal of Geotechnical and Geoenvironmental Engineering 143, 06016023.

Lawler, M.L., Farrell, E.R., Lochaden, A.L.E., 2010. Comparison of the measured and finite element–predicted ground deformations of a stiff lodgement till. Canadian Geotechnical Journal 48, 98-116.

Li, W., Afshani, A., Akagi, H., Oka, S., 2020. Influence of lining permeability and temperature on long-term behavior of segmented tunnel. Soils and Foundations 60, 425-438.

Li, Z., Soga, K., Kechavarzi, C., 2018. Distributed fibre optic sensing of a deep excavation adjacent to pre-existing tunnels. Géotechnique Letters 8, 171-177.

Li, Z., Soga, K., Wright, P., 2015. Long-term performance of cast-iron tunnel cross passage in London clay. Tunnelling and Underground Space Technology 50, 152-170.

Liu, B., Zhang, D.-W., Yang, C., Zhang, Q.-B., 2020. Long-term performance of metro tunnels induced by adjacent large deep excavation and protective measures in Nanjing silty clay. Tunnelling and Underground Space Technology 95, 103147.

Long, M., Menkiti, C.O., 2007. Geotechnical properties of Dublin Boulder Clay. Géotechnique 57, 595-611.

Mair, R.J., 2008. Tunnelling and geotechnics: new horizons. Géotechnique 58, 695-736.

Marshall, A.M., Farrell, R., Klar, A., Mair, R., 2012. Tunnels in sands: the effect of size, depth and volume loss on greenfield displacements. Géotechnique 62, 385-399.

Meguid, M.A., Dang, H.K., 2009. The effect of erosion voids on existing tunnel linings. Tunnelling and Underground Space Technology 24, 278-286.

Mohamad, H., Soga, K., Bennett Peter, J., Mair Robert, J., Lim Chi, S., 2012. Monitoring Twin Tunnel Interaction Using Distributed Optical Fiber Strain Measurements. Journal of Geotechnical and Geoenvironmental Engineering 138, 957-967.

Monsberger, C.M., Lienhart, W., 2021. Distributed fiber optic shape sensing along shotcrete tunnel linings: Methodology, field applications, and monitoring results. Journal of Civil Structural Health Monitoring 11, 337-350.

Mu, B., Xie, X., Li, X., Li, J., Shao, C., Zhao, J., 2021. Monitoring, modelling and prediction of segmental lining deformation and ground settlement of an EPB tunnel in different soils. Tunnelling and Underground Space Technology 113, 103870.

Ng, C.W.W., Liu, G.B., Li, Q., 2013. Investigation of the long-term tunnel settlement mechanisms of the first metro line in Shanghai. Canadian Geotechnical Journal 50, 674-684.

Ng, C.W.W., Wong, Y.Y.A., Shakeel, M., 2022. Effects of the skew angle of new tunneling on an existing tunnel: three-dimensional centrifuge and numerical modeling. Canadian Geotechnical Journal.

O'Brien, D., Andrew Osborne, J., Perez-Duenas, E., Cunningham, R., Li, Z., 2023. Automated crack classification for the CERN underground tunnel infrastructure using deep learning. Tunnelling and Underground Space Technology 131, 104668.

Rodenas-Herráiz, D.A.S., Kenichi%A Fidler, Paul R A%A de Battista, Nicholas, 2016. Wireless Sensor Networks for Civil Infrastructure Monitoring.

Sandrone, F., Labiouse, V., 2010. Analysis of the evolution of road tunnels equilibrium conditions with a convergence–confinement approach. Rock Mechanics and Rock Engineering 43, 201-218.

Shao, H., 2019. Analysis of deformation mechanism and wireless sensing method of shield tunnel for Shanghai Metro, College of Civil Engineering. Tongji University, Shanghai.

Showkati, A., Salari-rad, H., Hazrati Aghchai, M., 2021. Predicting long-term stability of tunnels considering rock mass weathering and deterioration of primary support. Tunnelling and Underground Space Technology 107, 103670.

Skipper, J., Follett, B., Menkiti, C.O., Long, M., Clark-Hughes, J., 2005. The engineering geology and characterization of Dublin Boulder Clay. Quarterly Journal of Engineering Geology and Hydrogeology 38, 171-187.

Soga, K., Kechavarzi, C., Pelecanos, L., De Battista, N., Williamson, M., Gue, C., Di Murro, V., Elshafie, M., 2017a. Distributed fibre optic strain sensing for monitoring underground structures - Tunnels Case Studies, Underground Sensing

pp. 287-321.

Soga, K., Laver, R.G., Li, Z., 2017b. Long-term tunnel behaviour and ground movements after tunnelling in clayey soils. Underground Space 2, 149-167.

Soga, K., Mohamad, Hisham, Bennett, Peter, J., 2008. Distributed fibre optics strain measurements for monitoring geotechnical structures, The Six international conference on case histories in geotechnical engineering.

Sui, Y., Cheng, X., Wei, J., 2021. Distributed fibre optic monitoring of damaged lining in double-arch tunnel and analysis of its deformation mode. Tunnelling and Underground Space Technology 110, 103812.

Usman, M., Galler, R., 2013. Long-term deterioration of lining in tunnels. International Journal of Rock Mechanics and Mining Sciences 64, 84–89.

Vanícek, I., Vanícek, M., Záleský, J., 2009. Monitoring of tunnel lining deformation and deterioration, in: al., M.H.e. (Ed.), Proceedings of the 17th International conference on soil mechanics and geotechnical engineering.

Wang, C., Friedman, M., Li, Z., 2020a. Time-dependent performance of Dublin Port Tunnel, Civil Engineering Research in Ireland 2020, Cork, Ireland, pp. 659-664.

Wang, C., Friedman, M., Li, Z., 2020b. Time-dependent performance of Dublin Port Tunnel, Civil Engineering Research Ireland 2020, Cork.

Wang, C., Friedman, M., Li, Z., 2021a. Hydraulic permeability and ageing behaviour of Dublin Port Tunnel, The 20th International Conference on Soil Mechanics and Geotechnical Engineering, Sydney.

Wang, C., Li, Z., Friedman, M., 2022a. Hydraulic permeability and ageing behaviour of Dublin Port Tunnel, 20th International Conference on Soil Mechanics and Geotechnical Engineering, Sydney, Australia.

Wang, F., Huang, H., Xue, Z.M., He, B., 2017. Wireless Sensing Method for Structural Behavior of Shield Tunnel. Zhongguo Gonglu Xuebao/China Journal of Highway and Transport 30, 222-228.

Wang, F., Shi, J., Huang, H., Zhang, D., Liu, D., 2021b. A horizontal convergence monitoring method based on wireless tilt sensors for shield tunnels with straight joints. Structure and Infrastructure Engineering 17, 1194-1209.

Wang, H., Huang, H., Feng, Y., Zhang, D., 2018. Characterization of Crack and Leakage Defects of Concrete Linings of Road Tunnels in China. ASCE-ASME Journal of Risk and Uncertainty in Engineering Systems, Part A: Civil Engineering 4, 04018041.

Wang, J., Zhang, J., Cohn, A.G., Wang, Z., Liu, H., Kang, W., Jiang, P., Zhang, F., Chen, K., Guo, W., Yu, Y., 2022b. Arbitrarily-oriented tunnel lining defects detection from Ground Penetrating Radar images using deep Convolutional Neural networks. Automation in Construction 133, 104044.

Wang, K., Xu, S., Zhong, Y., Han, Z., Ma, E., 2021c. Deformation failure characteristics of weathered sandstone strata tunnel: A case study. Engineering Failure Analysis 127, 105565.

WONGSAROJ, J., SOGA, K., MAIR, R.J., 2013. Tunnelling-induced consolidation settlements in London Clay. Géotechnique 63, 1103-1115.

Wood, A.M.M., 1975. The circular tunnel in elastic ground. Géotechnique 25, 115-127.

Wu, K., Cui, S., Liu, Y., Zhang, Q., Zhao, J., Zhang, Z., Han, Y., 2020. Study on the Mechanism of Grouting Under Different Tunnel Depth of Cross Passage. Geotechnical and Geological Engineering 38, 3291-3305.

Xie, X., Lu, X., 2017. Development of a 3D modeling algorithm for tunnel deformation monitoring based on terrestrial laser scanning. Underground Space 2, 16-29.

Xie, X., Zhang, D., Huang, H., 2018. Data Analysis of Shield Tunnel Deformation from Real-Time Monitoring with Wireless Sensing Network, International Conference: Tunnelling and Underground Construction, Shanghai, pp. 392-401.

Xie, X.Y., Feng, L., 2012. Real-Time Health Monitoring System for Power Tunnel. GeoCongress 2012, 3099-3108.

Xu, G., He, C., Chen, Z., Liu, C., Wang, B., Zou, Y., 2020. Mechanical behavior of secondary tunnel lining with longitudinal crack. Engineering Failure Analysis 113, 104543.

Yang, H., Xu, X., 2021. Structure monitoring and deformation analysis of tunnel structure. Composite Structures 276, 114565.

Yin, J., Huang, H., 2015. Real time monitoring method for the longitudinal settlement of shield tunnel using wireless inclinometer, Proceedings of the 2015 Information Technology and Mechatronics Engineering Conference. Atlantis Press, pp. 274-280.

Závacký, M., Chalmovský, J., Stefanak, J., Mica, L., Bílek, P., 2018. Modelling of tunnel lining degradation, 5th International Conference on Road and Rail Infrastructure, Zadar, Croatia, pp. 1499-1505.

Zhang, T., Taylor, R.N., Divall, S., Zheng, G., Sun, J., Stallebrass, S.E., Goodey, R.J., 2019. Explanation for twin tunnelling-induced surface settlements by changes in soil stiffness on account of stress history. Tunnelling and Underground Space Technology 85, 160-169.

Zheng, G., Tong, J., Zhang, T., Wang, R., Fan, Q., Sun, J., Diao, Y., 2020. Experimental study on surface settlements induced by sequential excavation of two parallel tunnels in drained granular soil. Tunnelling and Underground Space Technology 98, 103347.

Zhou, J., Xiao, H., Jiang, W., Bai, W., Liu, G., 2020. Automatic subway tunnel displacement monitoring using robotic total station. Measurement 151, 107251.

List of figures

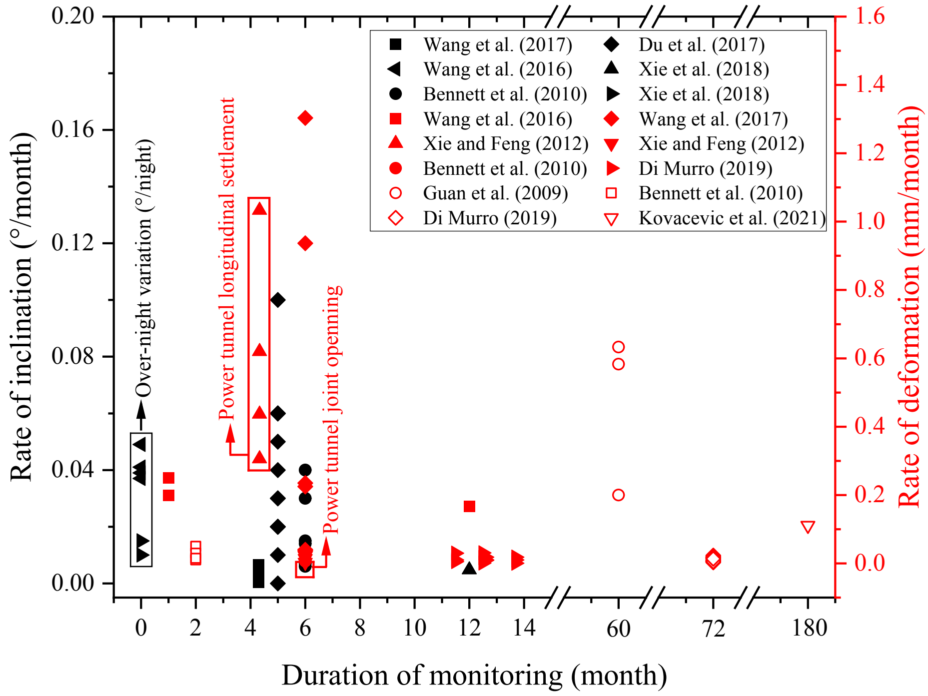

Figure 1. Rate of recorded inclination/convergence development

(a) Location of DPT

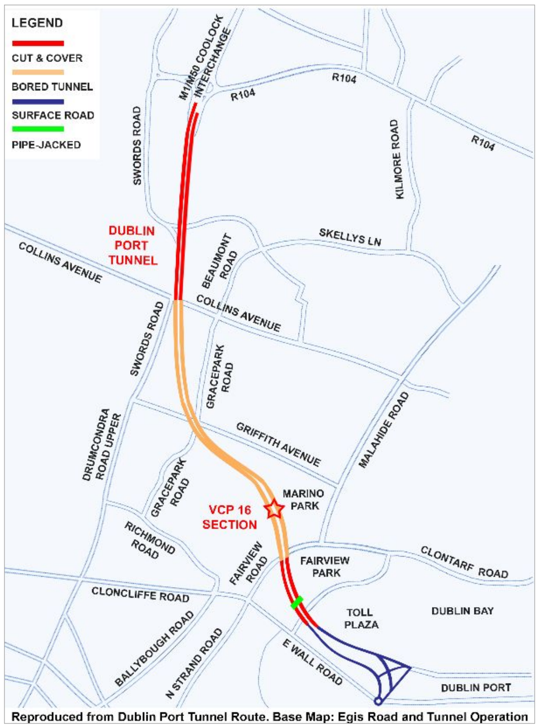

(b) Alignment of DPT

Figure 2. Location and alignment of Dublin Port Tunnel

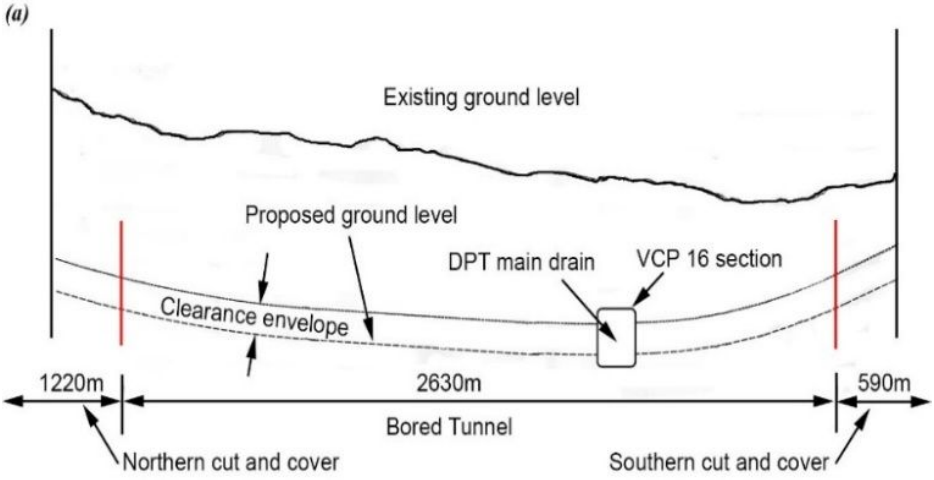

(*a*) Bored tunnel longitudinal alignment

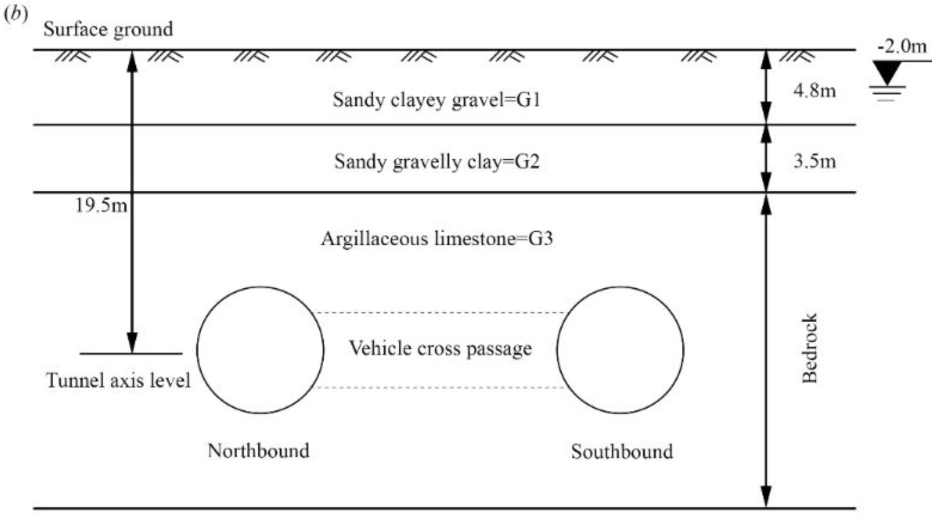

(*b*) Simplified geology around VCP 16

Figure 3. VCP 16 section geological profile

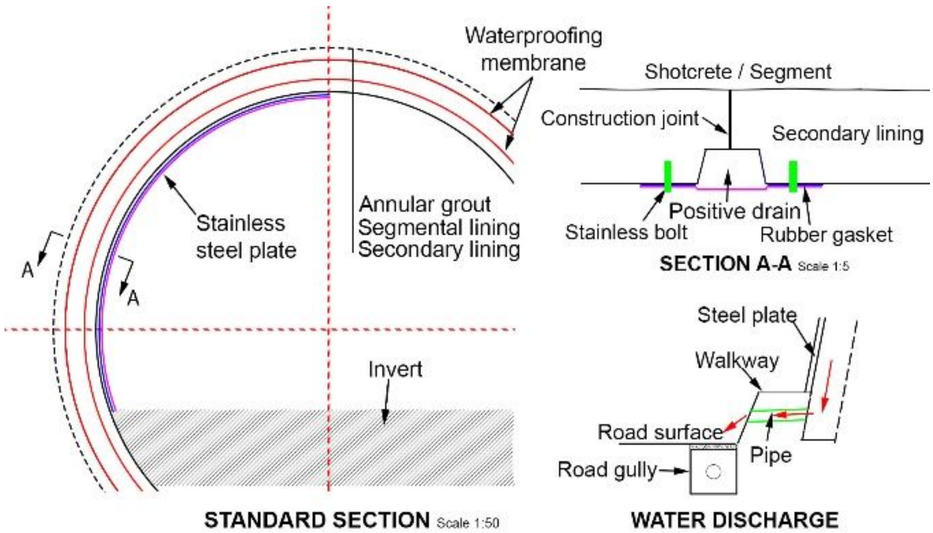

(a) DPT waterproofing and drainage system

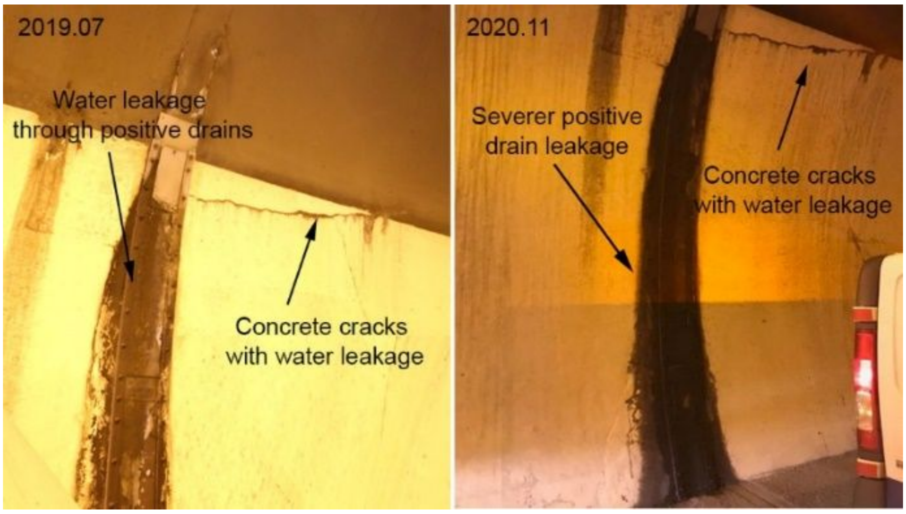

(b) VCP 16 section deterioration

Figure 4. DPT hydraulic profile

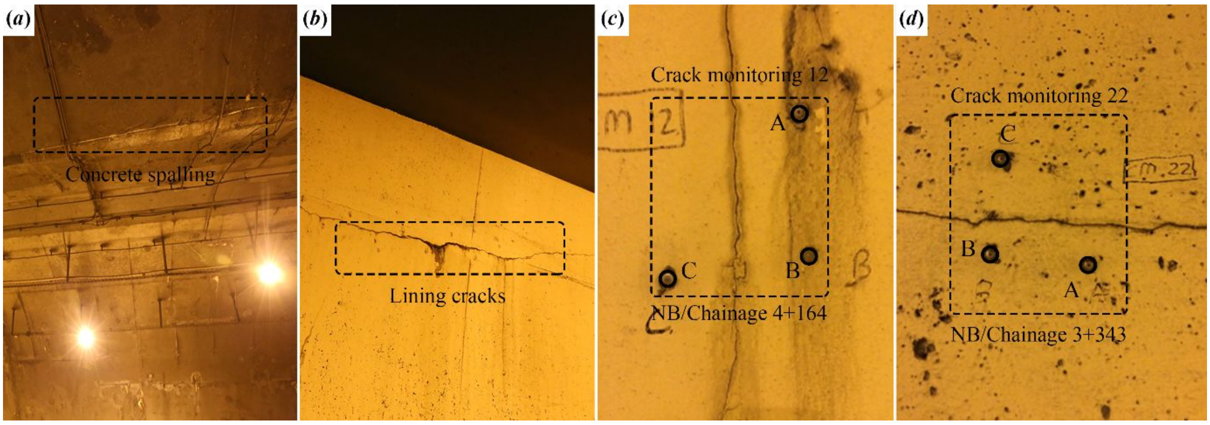

Figure 5. Existing crack monitoring

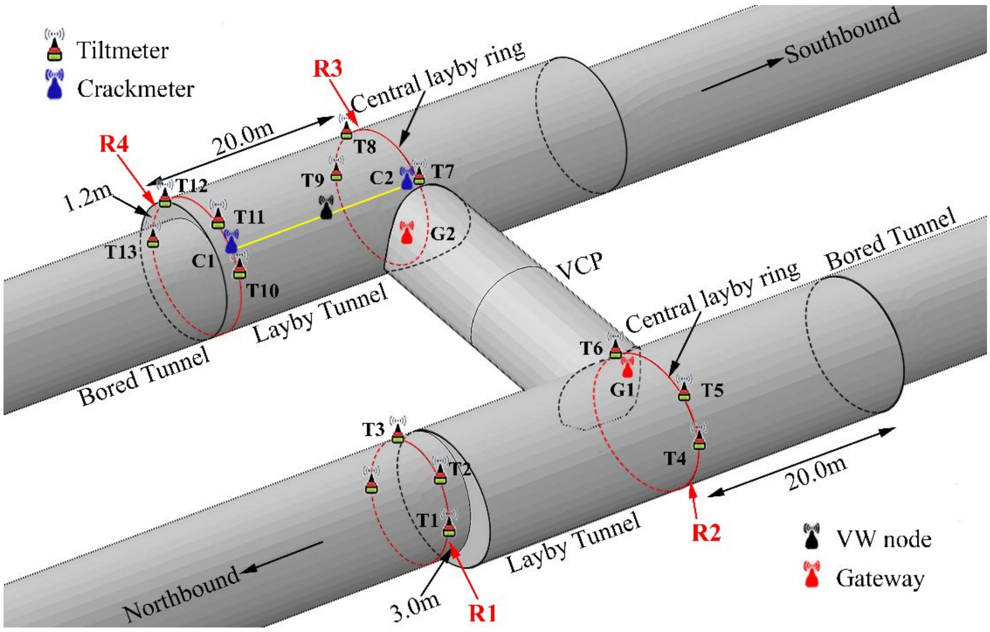

(a) sensor deployment illustration

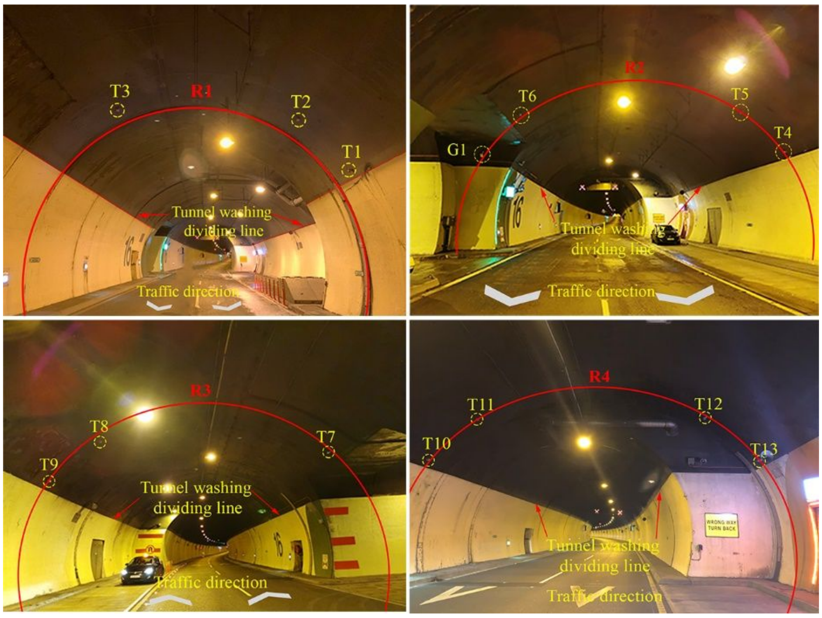

(b) onsite sensor deployment

Figure 6. WSN sensor deployment

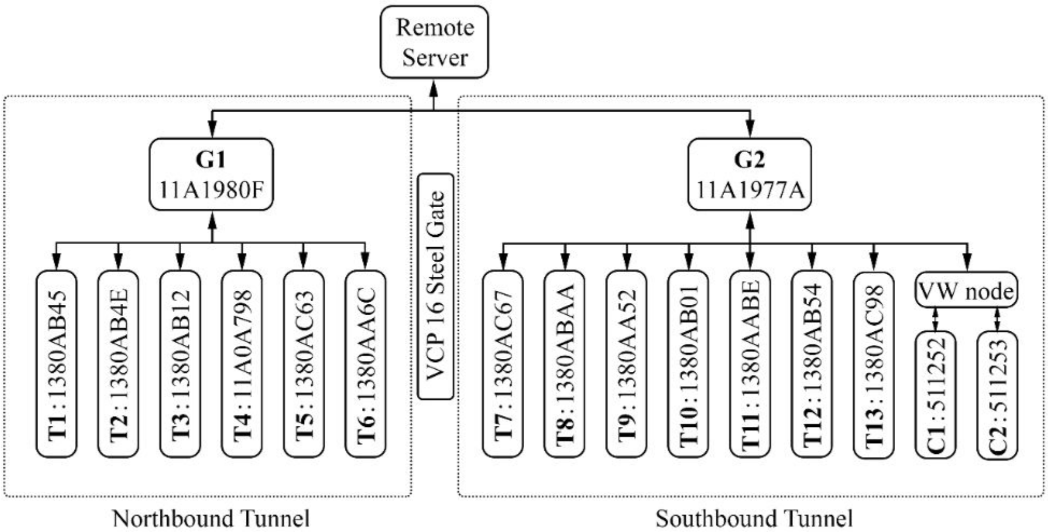

Figure 7. WSN star topology in Dublin Port Tunnel

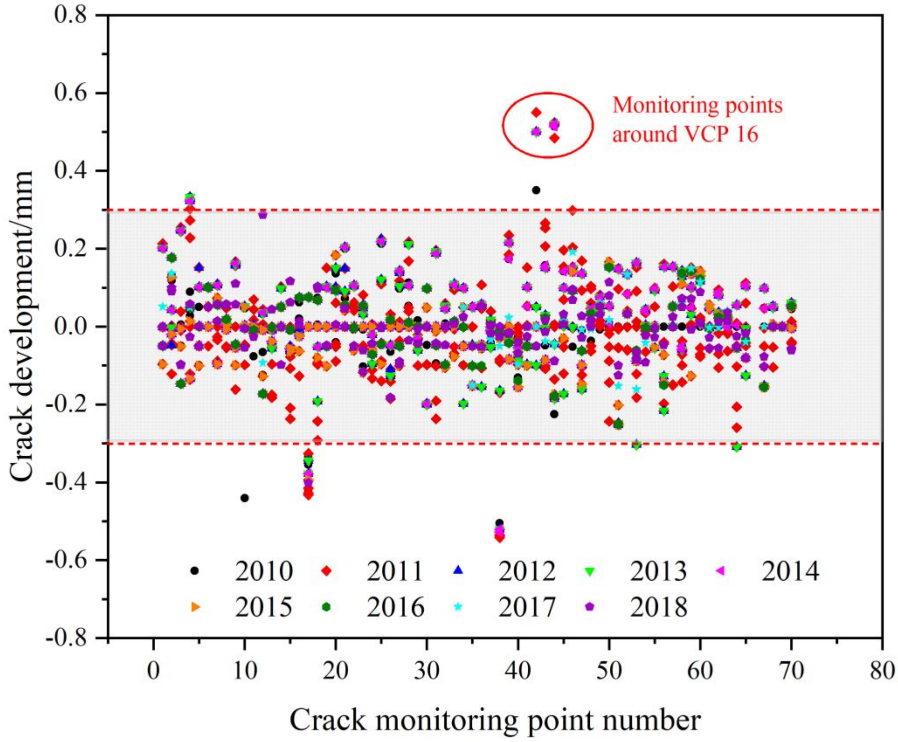

Figure 8. Crack development from existing monitoring

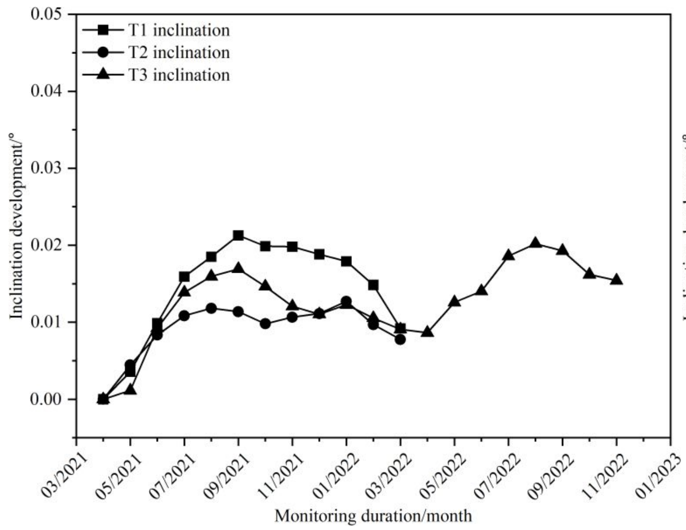

(*a*) R1 inclination development

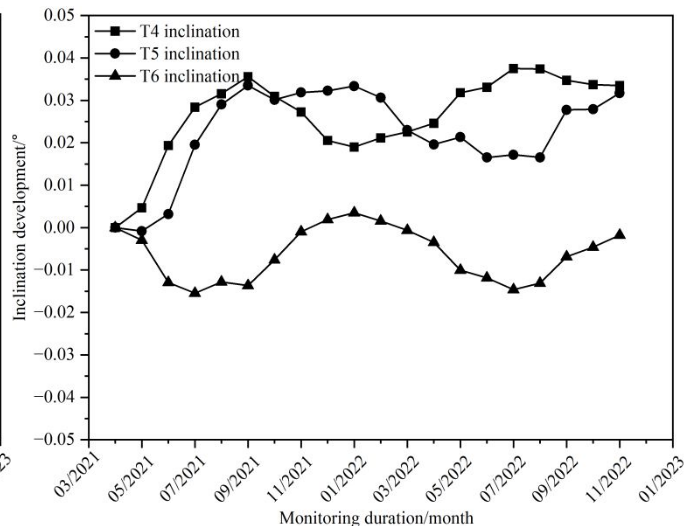

(*b*) R2 inclination development

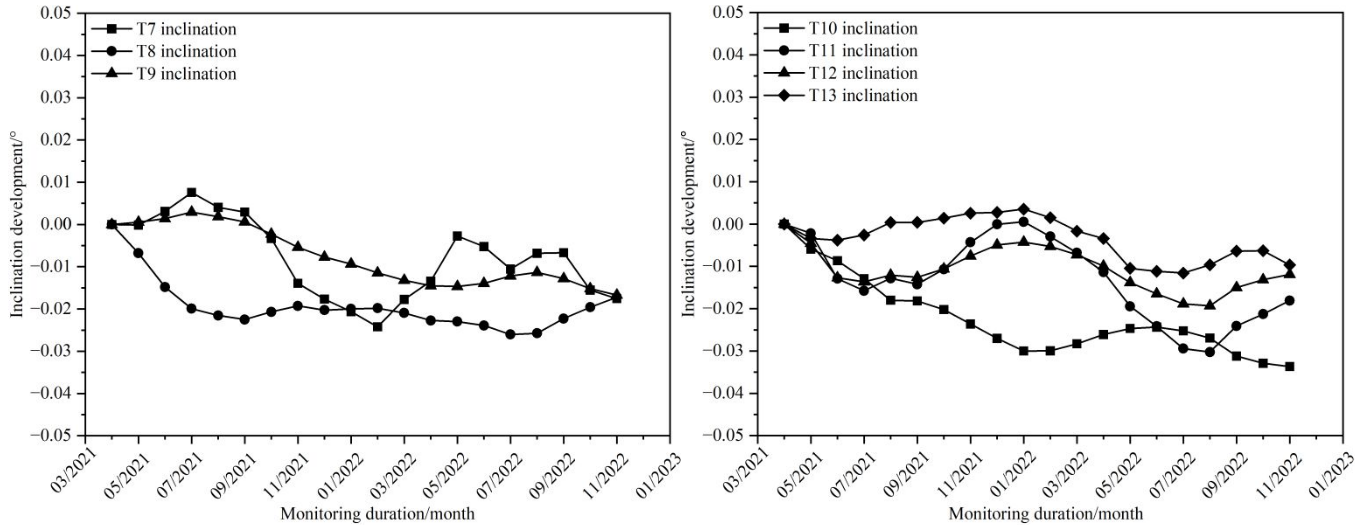

(*c*) R3 inclination development (*d*) R4 inclination development

Figure 9. Tunnel inclination development with time (monthly increment)

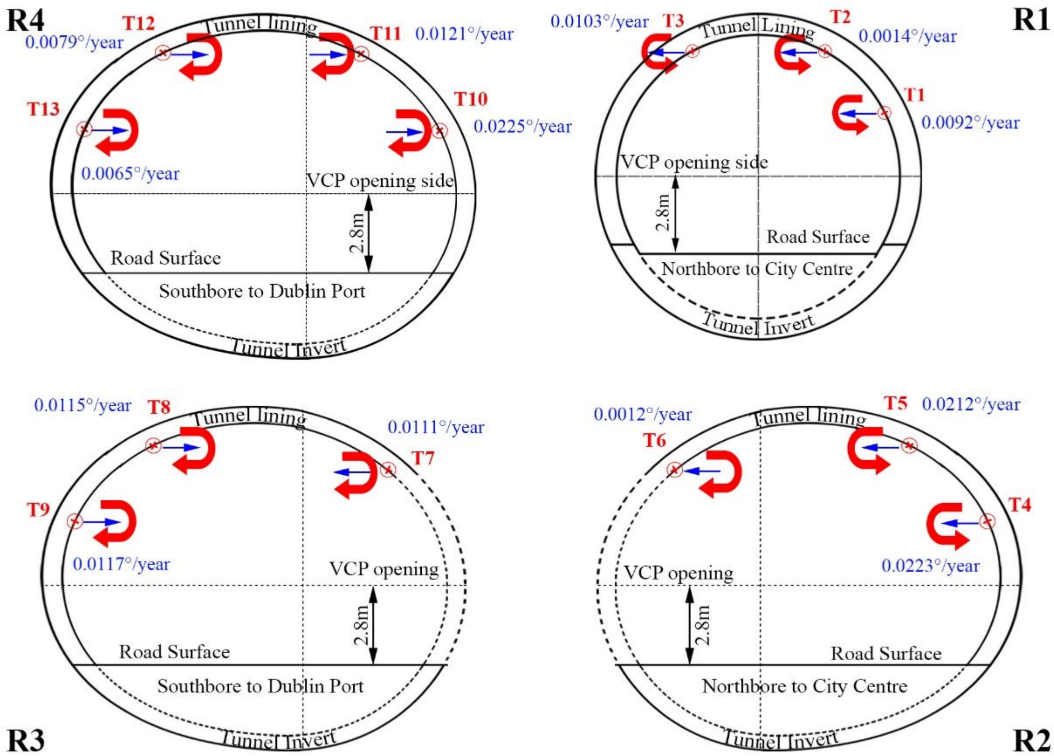

Figure 10. Rate of tunnel inclination

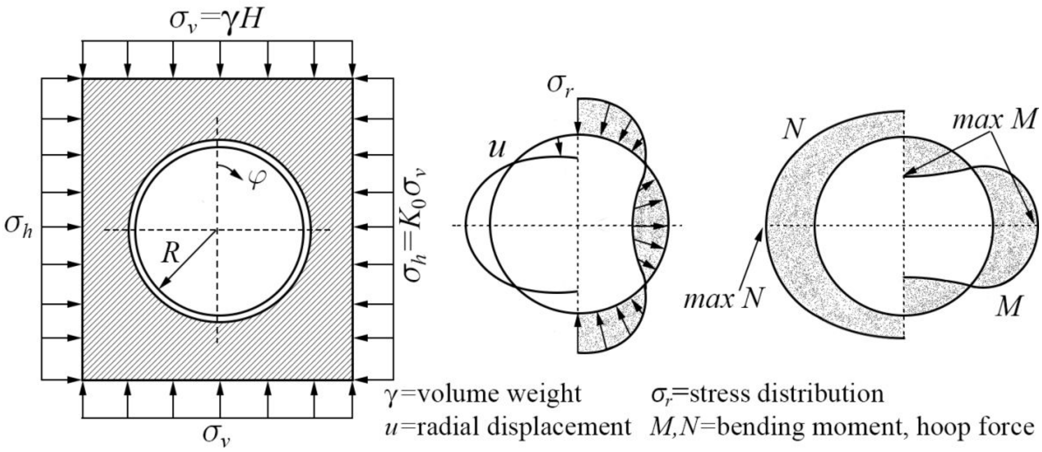

Figure 11. Plain strain continuum model

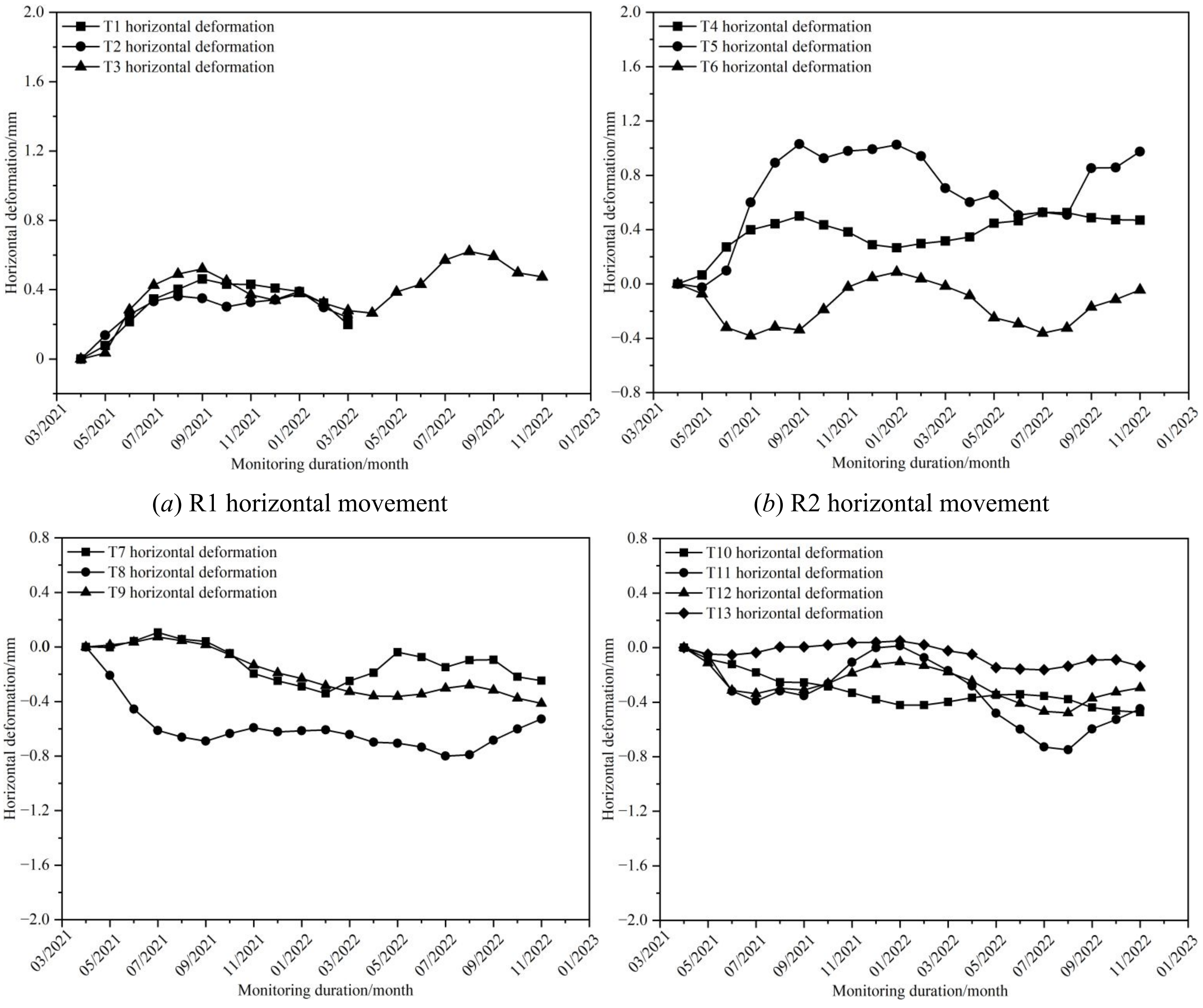

(*a*) R1 horizontal movement (*b*) R2 horizontal movement

(*c*) R3 horizontal movement (*d*) R4 horizontal movement

Figure 12. Converted horizontal displacement of sensing locations with time (monthly increment)

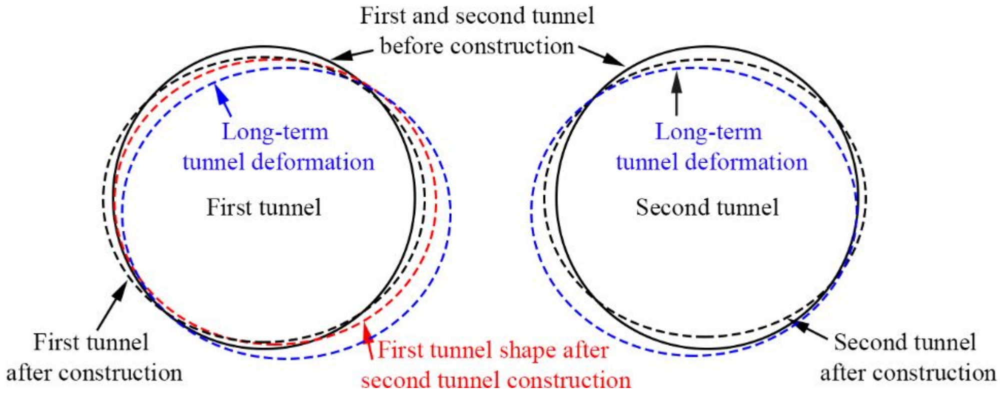

(*a*) Tunnel deformation under twin tunnel effect

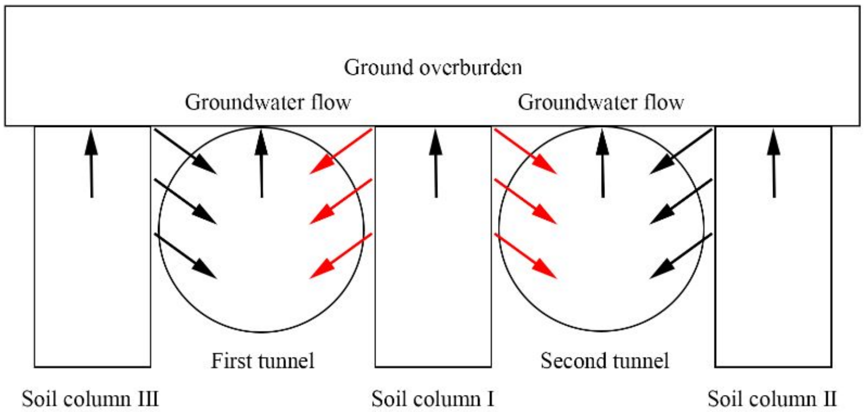

(*b*) Twin tunnel interaction in the long term

Figure 13. Twin tunnel effect

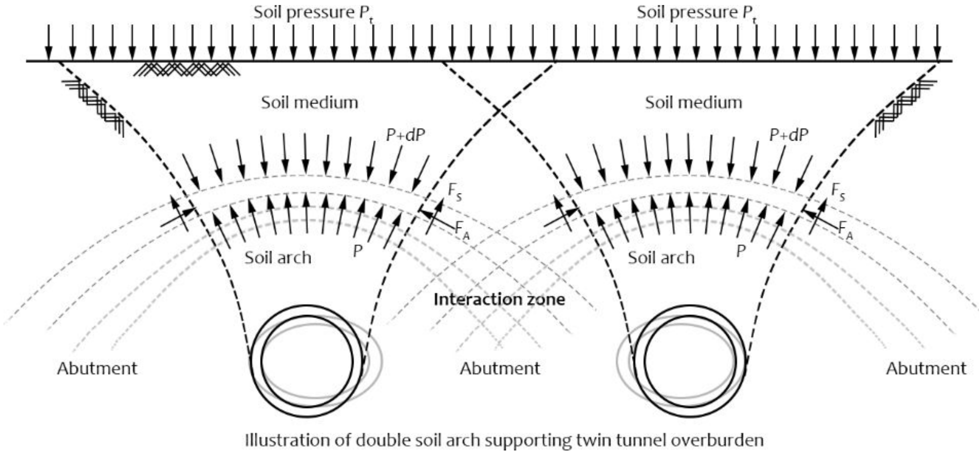

(*a*) Twin tunnel arching effect

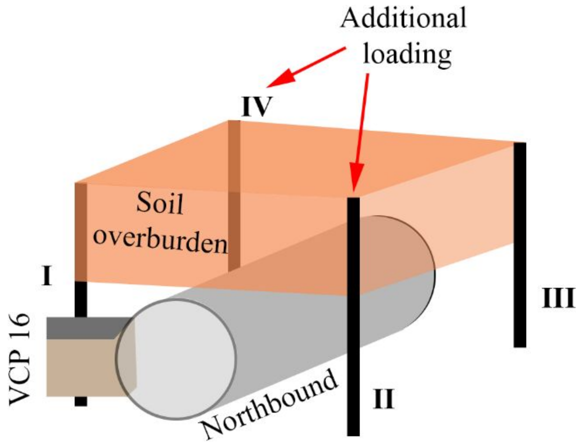

(*b*) “Table” load column analogy

Figure 14. Illustration of VCP effect

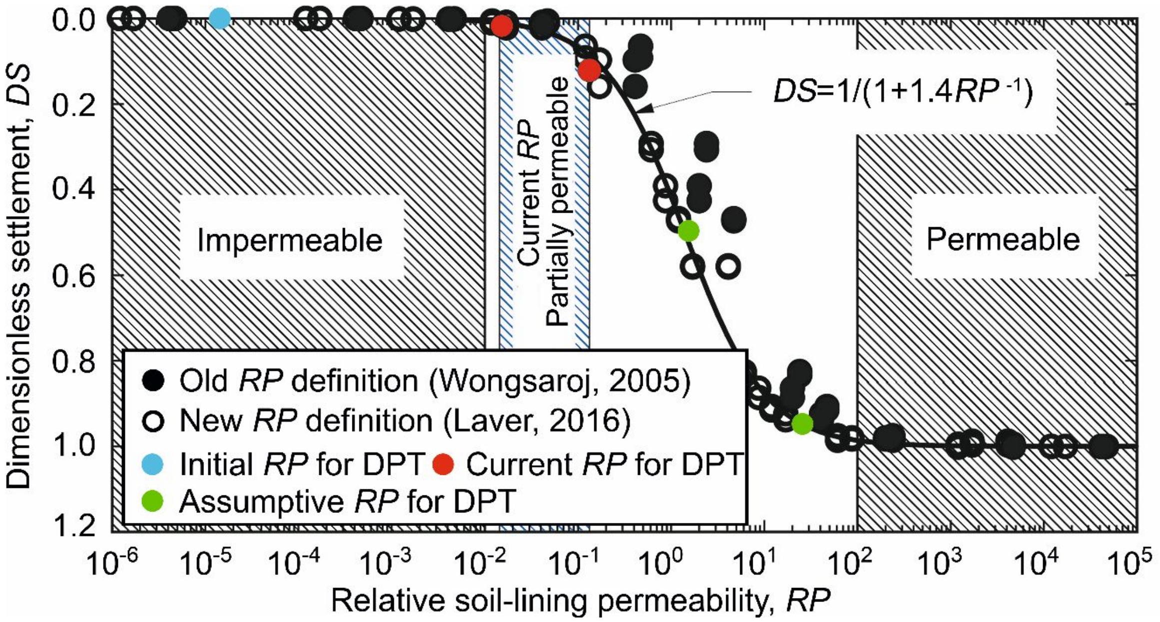

(*a*) *RP* for DPT vs. *DS* (Wang et al., 2022a)

(*b*) Layby lining crack distribution

Figure 15. (*a*) RP for DPT vs. DS; (*b*) Layby lining crack distribution

List of tables

Table 1. Representative cases of long-term tunnel performance monitoring

Literature	Tunnel type and configuration	Monitoring motivation	Method	Duration	Characteristics	Monitoring items	Data collection
Guan et al. (2009)	Single cast-in-situ concrete mountain tunnel	Influence of surrounding ground deterioration on tunnel performance	ATS	60 months (1992-1997)	Non-real time and discrete point monitoring	Lining crown, invert and spring-line deformation	ATS: Automatic storage but manual retrieval
Kovačević et al. (2021)	Single cast-in-situ concrete road tunnel	Influence of surrounding soft rock on the long-term tunnel performance	MP	15 years (2005-2019)	Non-real time and discrete point monitoring	Lining crown settlement with time	Manual reading and collection
Mohamad et al. (2012)	Single segmental concrete tunnel of a twin tunnel system	Influence of the adjacent excavation of a second tunnel on the existing one	DFOS	45 days (25.10.2006-08.12.2006)	Spatially continuous measurement	Circumferential strains	Automatic collection but manual retrieval
Gue et al. (2015)	Single segmental cast-iron tunnel with a new one underneath	Influence of the excavation of the tunnel underneath on the one above	DFOS	11 months (16.04.2013-14.03.2014)	Spatially continuous measurement	Circumferential and longitudinal strains	Automatic collection but manual retrieval
Soga et al. (2017a)	Single SCL tunnel of a tunnel junction (three tunnels)	Influence of the excavations of two cross passages on the parent tunnel	DFOS	≈ 3 months (06.2014-08.2014)	Spatially continuous measurement	Cross-sectional and longitudinal strains	Automatic collection but manual retrieval
Li et al. (2018)	Diaphragm wall of a station tunnel deep excavation	Effect of a pre-existing tunnel on diaphragm wall behaviour	DFOS	During tunnel passage, concourse excavation	Spatially continuous measurement	Mechanical and thermal strain	Automatic collection but manual retrieval
Di Murro (2019)	Single inclined SCL tunnel of a complexed tunnel system	Effect of tunnel deteriorations on the stress conditions of an existing tunnel	DFOS ATS	6 years (07.2013-10.2019)	Spatially continuous (DFOS) DP measurement (ATS)	Strain (DFOS) Convergence (ATS)	Automatic (DFOS) and manual collection (ATS)
Vanícek et al. (2009)	Single double-track metro tunnel of Line C Prague Metro	Effect of tunnel deteriorations on the stability of the existing tunnel	WSN	From the end of 2016	Real-time and temporally continuous measurement	Convergence and inclination	Automatic collection and remote retrieval
Yin and Huang (2015)	Not Applicable	Influence of longitudinal settlement on tunnels' longitudinal performance	WSN	Not Applicable	Real-time and temporally continuous measurement	Longitudinal inclination (convergence)	Automatic collection and remote retrieval
Wang et al. (2017)	Single shield tunnel of a twin tunnel system	Influence of adjacent excavation on close-by tunnel performance	WSN	≈ 6 months (01.11.2015-30.04.2016)	Real-time and temporally continuous measurement	Inclination, longitudinal settlement, seepage, etc.	Automatic collection and remote retrieval
Xie et al. (2018)	Single shield tunnel of a twin tunnel system	Impact of adjacent soil unloading on close-by shield tunnel performance	WSN	500 days (18.10.2015-15.02.2017)	Real-time and temporally continuous measurement	Circumferential inclination convergence)	Automatic collection and remote retrieval
Bennett et al. (2010a)	Single expanded concrete tunnel of Jubilee Line, London Underground	Assess the risk of lining movement due to tunnel ageing and deterioration	WSN VWSG	≈ 6 months (07.2008-01.2009)	Real-time (WSN) non-real-time (VWSG) and DP-based	Inclination, joint and crack development	Automatic (WSN) Manual (VWSG)
Xie and Feng (2012)	A single concrete-lined power tunnel	Influence of hydraulic and structural deteriorations on tunnel performance	WSN	224 days (27.04.2010-07.12.2010)	Real-time and temporally continuous measurement	Differential settlement and joint opening	Automatic collection and remote retrieval
Wang et al. (2021b)	Single shield tunnel of a twin tunnel system	Adjacent excavation and grouting reinforcement on tunnel performance	WSN ATS	40 days in excavation (16.07.2014-24.08.2014) 260 days after grouting (25.08.2014-12.05.2015)	Real-time (WSN) non-real-time (ATS) and DP-based	Circumferential inclination and converted convergence	WSN: Automatic collection and retrieval ATS: Automatic storage but manual retrieval
Lai et al. (2015)	A single road tunnel with angled undercrossing new tunnel	Effect of the blast-induced vibration on the structure of existing tunnel above	WSN	During the construction of the new tunnel below	Real-time and temporally continuous measurement	Vibration, concrete strain, peak particle velocity	Automatic collection and remote retrieval

Note: 1. The table lists representative applications that have been published so far of both traditional and the other two advanced methods into monitoring the long-term performance of tunnels; 2. Abbreviations: ATS – Automatic total station; VWSG –Vibrating wire strain gauge; DP – discrete point; SCL – sprayed concrete lining; MP – measurement pipe.

Table 2. List of WSN nodes

Tunnel	WSN node				Total
	Inclinometer	Crack-meter	VW interface node	Gateway	
Southbound	6	2	1	1	18
Northbound	7	0	0	1	